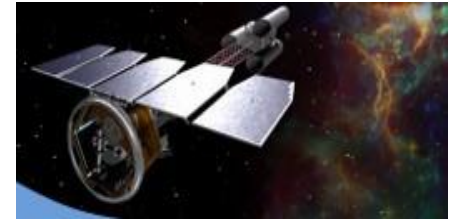




IXPE

Imaging
X-Ray
Polarimetry
Explorer



Science with the Imaging X-ray Polarimetry Explorer

Giorgio Matt (Univ. Roma Tre, Italy)



IXPE

Imaging
X-Ray
Polarimetry
Explorer

INTRODUCTION

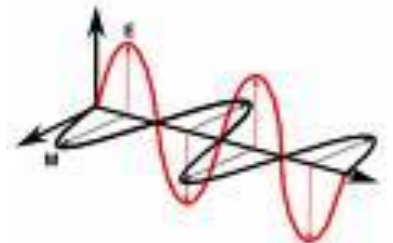
Information on celestial (extra-solar) sources are mostly provided by electromagnetic radiation.

They can be obtained by studying the spatial, spectral, timing and *polarization* properties of the observed radiation.

In particular, the polarization properties give us information on *geometry* (in a broad sense: geometry of the emitting matter but also of magnetic and gravitational fields, of space-time, etc.): the polarization degree depends on the level and type of symmetry of the system, the polarization angle indicates its orientation.

Our knowledge of the emission from a celestial source in any energy band is therefore incomplete without polarimetry.

However, polarimetric informations of astrophysical sources are basically missing in the X-ray band !





IXPE

Imaging
X-Ray
Polarimetry
Explorer

INTRODUCTION

Polarimetry has proved very important in radio, IR and optical bands (eg. jet emission in blazars, Unification Model of AGN, ...).

In *X-rays*, where non-thermal emission processes and aspherical geometries are likely to be more common than at lower energies, polarimetry is expected to be vital to fully understand emitting sources.

However, only one measurement ($P=19\%$ for the Crab Nebula, indicating synchrotron emission) has been obtained so far, together with a tight upper limit to Sco X-1.

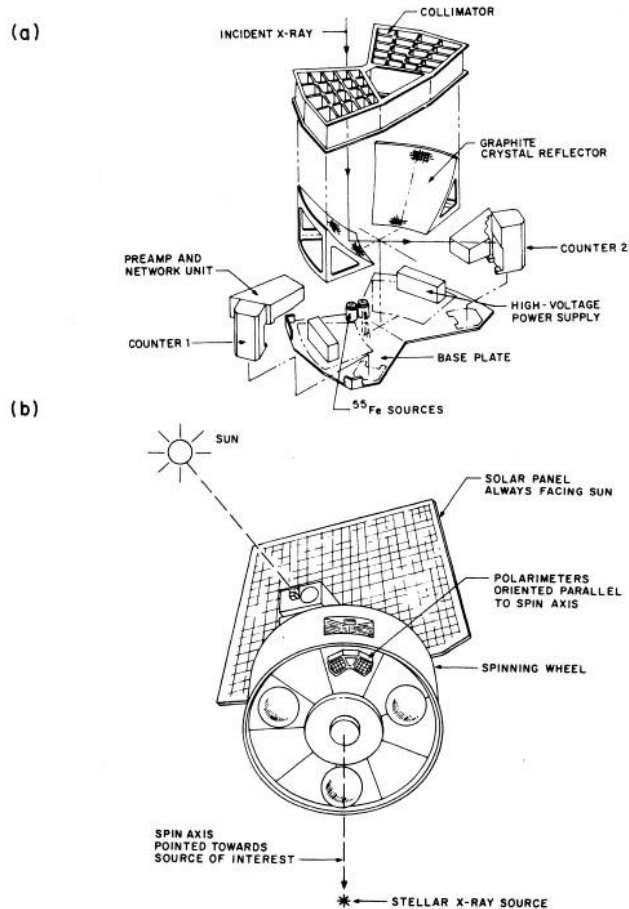


FIG. 1.—(a) Exploded view of the OSO-8 polarimeter assemblies. (b) Location of the polarimeters in the satellite.

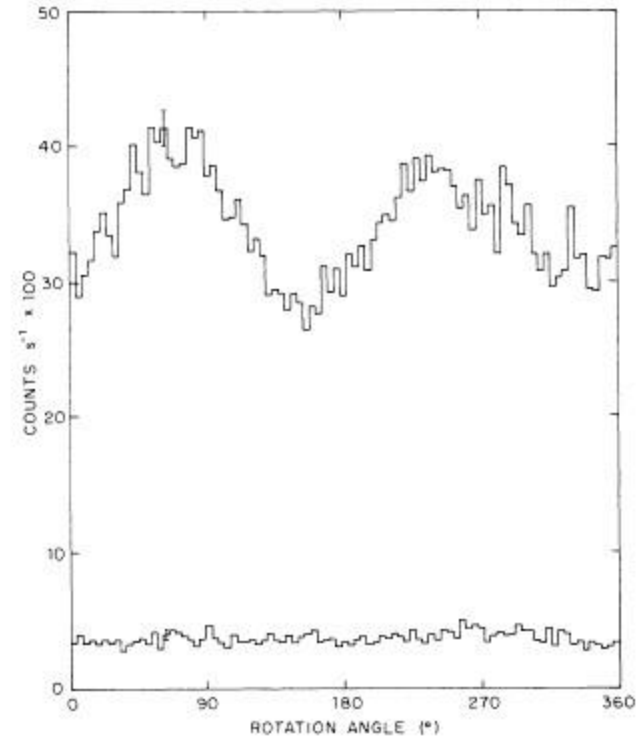


FIG. 2.—Average modulation curves obtained with both detectors at 2.6 keV during (*upper curve*) observations of the Crab Nebula and during (*lower curve*) observations of the Earth-occulted instrumental background.



IXPE

Imaging
X-Ray
Polarimetry
Explorer

INTRODUCTION

Polarimetry has proved very important in radio, IR and optical bands (eg. jet emission in blazars, Unification Model of AGN, ...).

In *X-rays*, where non-thermal emission processes and aspherical geometries are likely to be more common than at lower energies, polarimetry is expected to be vital to fully understand emitting sources.

However, only one measurement ($P=19\%$ for the Crab Nebula, indicating synchrotron emission) has been obtained so far, together with a tight upper limit to Sco X-1.

These measurements have been obtained in the 70s, for the two brightest sources in the X-ray sky.

The lack, for many decades, of significant technical improvements implied that no polarimeters were put on board of X-ray satellites.



IXPE

Imaging
X-Ray
Polarimetry
Explorer

INTRODUCTION

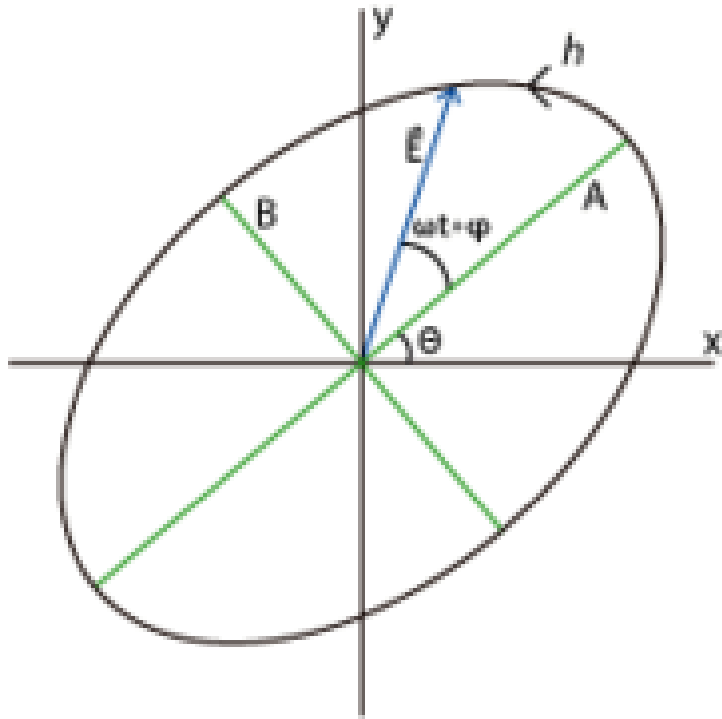
The situation has changed dramatically with the advent of polarimeters based on the photoelectric effect. Such detectors, on the focal plane of a X-ray telescope, may provide astrophysically interesting measurements for hundreds of sources (remember that polarimetry is a photon hungry technique...). The brightest specimens of all major classes of X-ray sources are now accessible!

Time is ripe for a X-ray polarimetric mission !

And, indeed, the Imaging X-ray Polarimetry Explorer (IXPE) has been selected in the NASA SMEX program for a launch in 2021

IXPE will perform spectrally-, spatially- and time-resolved polarimetry of hundreds of celestial sources to provide a breakthrough in astrophysics and fundamental physics

POLARIZATION



The polarization vector (which is a *pseudovector*, i.e. modulus π) rotates forming an ellipse. Polarization is described by the *Stokes parameters*:

$$I = A^2 + B^2$$

$$Q = (A^2 - B^2) \cos 2\theta$$

$$U = (A^2 - B^2) \sin 2\theta$$

$$V = \pm 2AB$$

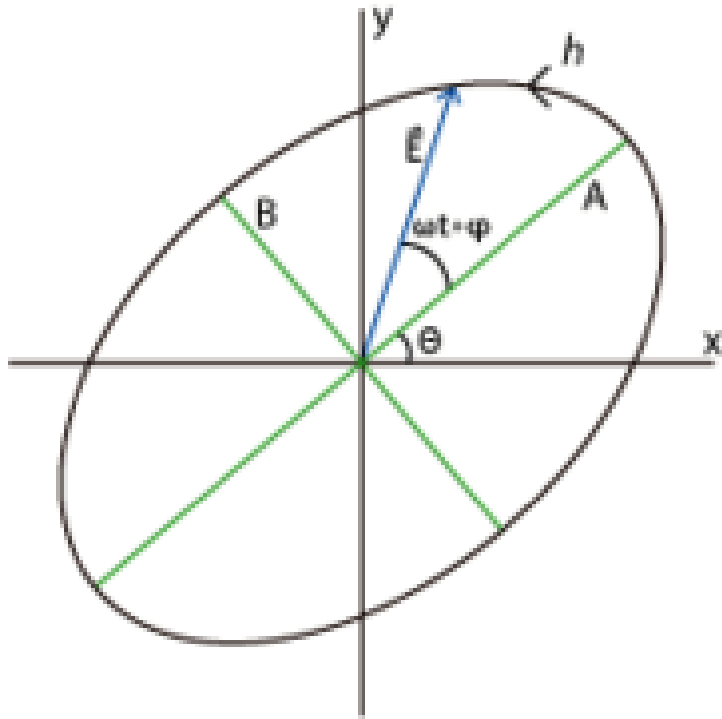
$$(I = \sqrt{Q^2 + U^2 + V^2})$$

100% Q	100% U	100% V
<p>+Q</p> <p>$Q > 0; U = 0; V = 0$ (a)</p>	<p>+U</p> <p>$Q = 0; U > 0; V = 0$ (c)</p>	<p>+V</p> <p>$Q = 0; U = 0; V > 0$ (e)</p>
<p>-Q</p> <p>$Q < 0; U = 0; V = 0$ (b)</p>	<p>-U</p> <p>$Q = 0; U < 0; V = 0$ (d)</p>	<p>-V</p> <p>$Q = 0; U = 0; V < 0$ (f)</p>

If $V=0$, radiation is **linearly polarized**

If $Q=U=0$, radiation is **circularly polarized**

POLARIZATION



Summing up the contributions of all photons, I increases while this is not necessarily so for the other Stokes parameters. Therefore:

$$I_T \geq \sqrt{Q_T^2 + U_T^2 + V_T^2}$$

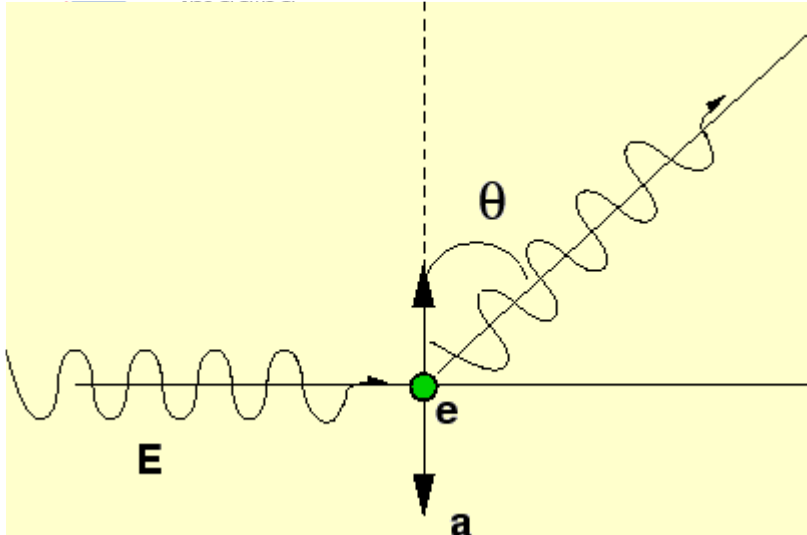
The net polarization degree and angle are given by:

$$\Pi = \frac{\sqrt{Q_T^2 + U_T^2 + V_T^2}}{I_T}$$

$$\chi = \frac{1}{2} \arctan \frac{U_T}{Q_T}$$

100% Q	100% U	100% V
<p>+Q</p> <p>$Q > 0; U = 0; V = 0$ (a)</p>	<p>+U</p> <p>$Q = 0; U > 0; V = 0$ (c)</p>	<p>+V</p> <p>$Q = 0; U = 0; V > 0$ (e)</p>
<p>-Q</p> <p>$Q < 0; U = 0; V = 0$ (b)</p>	<p>-U</p> <p>$Q = 0; U < 0; V = 0$ (d)</p>	<p>-V</p> <p>$Q = 0; U = 0; V < 0$ (f)</p>

THOMSON SCATTERING



It is the interaction between a photon and an electron (at rest), with $h\nu \ll mc^2$. It is an elastic process. The cross section is:

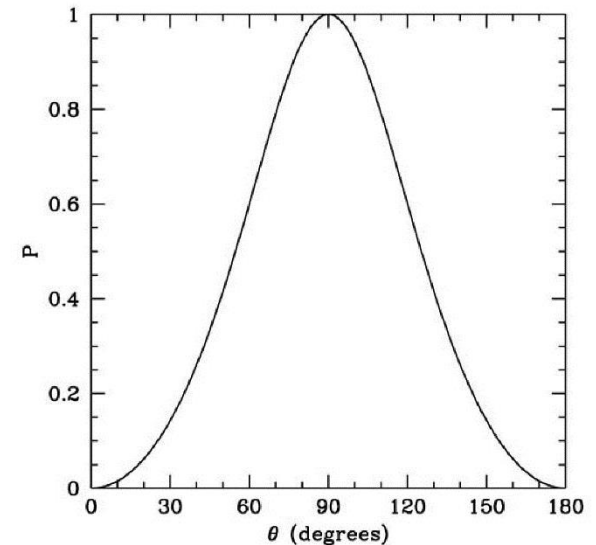
$$\sigma_T = \frac{8\pi e^2}{3m^2 c^4} = 6.65 \times 10^{-25} \text{ cm}^2$$

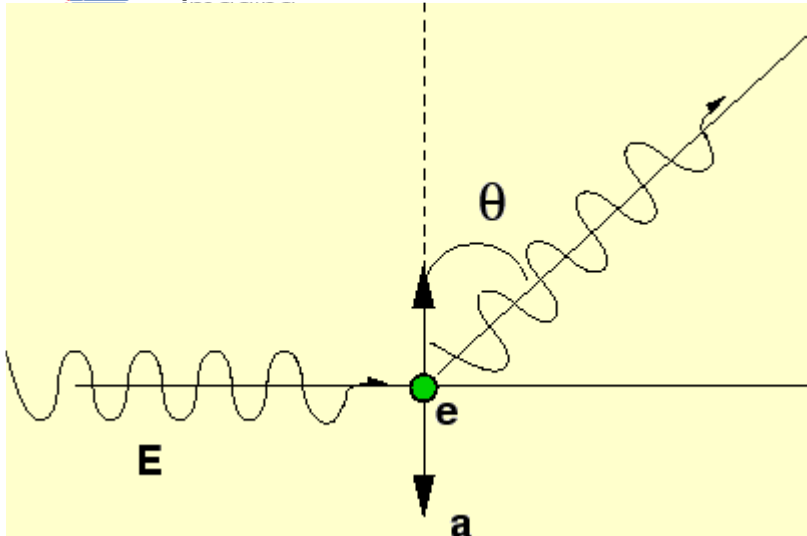
The differential cross section is:

$$\frac{d\sigma_T}{d\Omega} = \frac{e^4}{m^2 c^4} \sin^2 \theta$$

The scattered radiation is polarized. A 100% polarized beam gives rise to a 100% polarized scattered radiation, independently of the scattering angle. The polarization degree of a parallel beam of unpolarized radiation is:

$$P = \frac{1 - \cos^2 \theta}{1 + \cos^2 \theta}$$





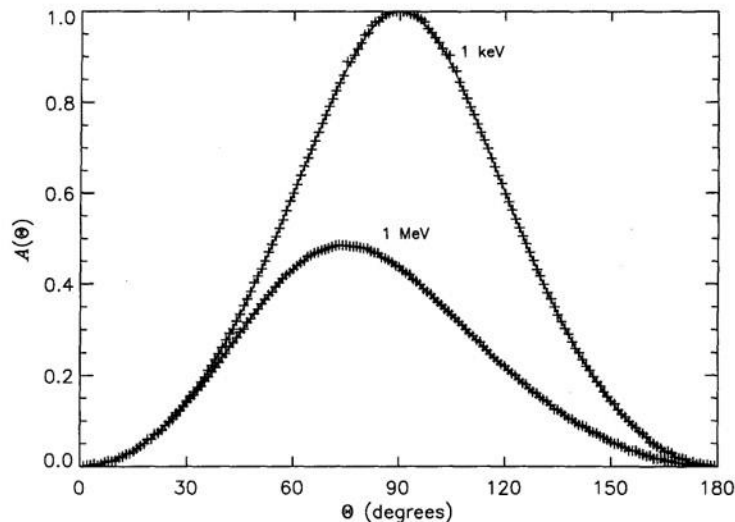
COMPTON SCATTERING

Compton scattering radiation is polarized (*but less than Thomson scattering. Polarization degree decreases with $h\nu/mc^2$ in the reference frame of the electron*). A 100% polarized beam gives rise to <100% polarized scattered radiation, depending on the scattering angles.

For an unpolarized beam, maximum polarization is less than 100%.

410

Giorgio Matt *et al.*





IXPE

Imaging
X-Ray
Polarimetry
Explorer

BREMSSTRAHLUNG

Bremsstrahlung photons are polarized with the electric vector perpendicular to the plane of interaction.

In most astrophysical situations, and certainly in case of thermal bremsstrahlung, the planes of interaction are randomly distributed, resulting in **null net polarization.**

For an anisotropic distribution of electrons, however, bremsstrahlung emission can be polarized.

SYNCHROTRON EMISSION

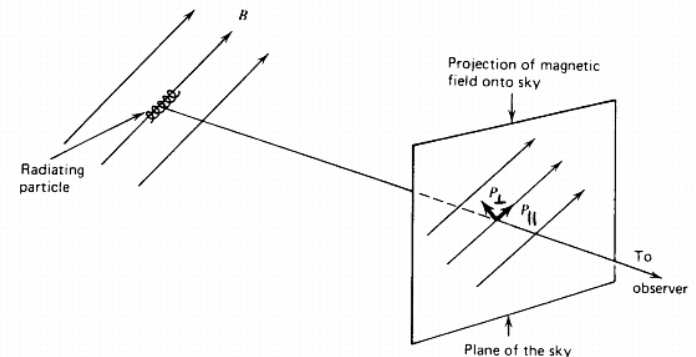


The radiation is polarized perpendicularly to the projection of B on the sky

For a power law distribution of emitting particles, the degree of polarization is

$$\Pi = (p+1)/(p+7/3).$$

This is actually an upper limit, because the magnetic field is never perfectly ordered.





IXPE

Imaging
X-Ray
Polarimetry
Explorer

IXPE'S TIMELINE

- **Proposed to NASA as a SMAll EXplorer (SMEX) mission in December 2014**
- **One of the three proposals selected for an Assessment Study in August 2015**
- **Final down-selection in January 2017**
- **Launch on early 2021**
- **Baseline duration: 2 years**



IXPE

Imaging
X-Ray
Polarimetry
Explorer

IXPE WILL:

▪ **(Re)Open the X-ray polarimetry window**

- Only one positive measurement so far: 19% polarization of the Crab Nebula (OSO-8)

▪ **Address key scientific questions**

- What is the spin of a black hole?
- What are the geometry and magnetic-field strength in magnetars?
- Was our Galactic Center an Active Galactic Nucleus in the recent past?
- What is the magnetic field structure in synchrotron X-ray sources?
- What are the geometries and origins of X-rays from pulsars (isolated and accreting)?
-

▪ **Provide powerful and unique capabilities**

- Integration time reduced by a factor of 100 over OSO-8 experiment
- Simultaneous imaging, spectroscopic, timing, and polarization data
- Instrument systematic effects at less than a fraction of a percent
- Meaningful polarization measurements for a large number of sources of different classes



IXPE

Imaging
X-Ray
Polarimetry
Explorer

IXPE

Principal Investigator: **M. C. Weisskopf (MSFC)**

Co-Investigators: *Brian D. Ramsey, Paolo Soffitta, Ronaldo Bellazzini, Enrico Costa, Stephen L. O'Dell, Allyn Tennant, Herman Marshall, Fabio Muleri, Jeffery Kolodziejczak, Roger W. Romani, Giorgio Matt, Victoria Kaspi, Ronald Elsner, L. Baldini, L. Latronico*

 <p>Marshall Space Flight Center</p> <p>PI team, project management, SE and S&MA oversight, mirror module fabrication, X-ray calibration, science operations, and data analysis and archiving</p>	 <p>Polarization-sensitive imaging detector systems</p>
 <p>Detector system funding, ground station</p>	 <p>Mission operations</p>
 <p>Spacecraft, payload structure, payload, observatory I&T</p>	 <p>Scientific theory</p>  <p>Science Working Group Co-Chair</p>  <p>Massachusetts Institute of Technology</p> <p>Co-Investigator</p> <p>A12567_151</p>

- Pegasus XL launch from Kwajalein
- 540-km circular orbit at 0° inclination
- 2 year baseline mission, 1 year SEO
- Point-and-stare at known targets
- Science Operations Center at MSFC
- Mission Operations Center at CU/LASP
- Malindi ground station (Singapore Backup)



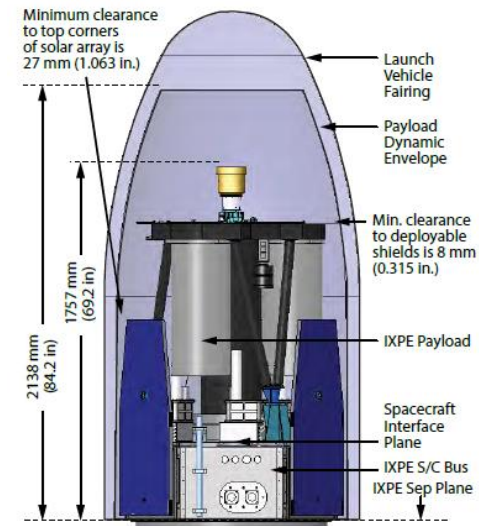
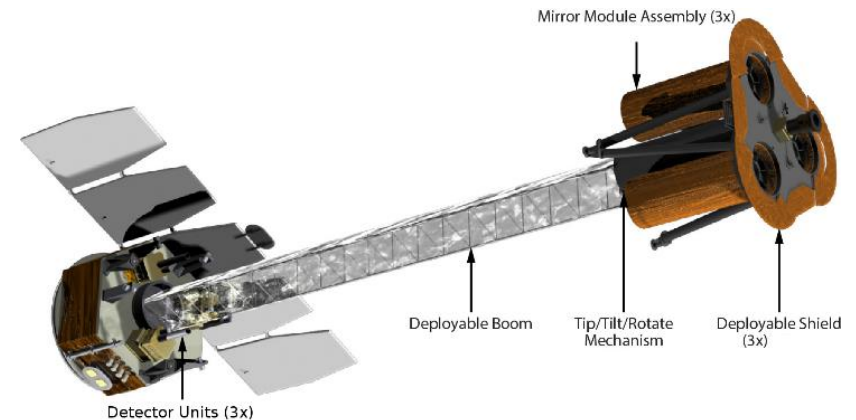
Science Advisory Team

■ 3x Telescopes

- 3x Mirror Units (MUs) + 3x Detector Units (DUs)
- A Detectors Service Unit (DSU) with built-in redundancy
- 4 m focal length, deployable boom and X-ray shield

■ Performance

- Polarization sensitivity: $MDP_{99\%} < 5.5\%$ in 1 day for flux of 10^{-10} ergs/cm²/sec
- Energy range: 2-8 keV
- Limit polarization: 0.5% (degree), 1 degree (angle)
- Angular resolution: better than 30 arcsec, field of view larger than 9 arcmin
- UTC synchronization: better than 250 μ s
- Energy resolution: better than 25%





IXPE

Imaging
X-Ray
Polarimetry
Explorer

SCIENCE ADVISORY TEAM ***(chairs: R. Romani & G. Matt)***

- PWN & Isolated pulsars

N. Bucciantini - INAF

- SNR

P. Slane - Harvard

- Accreting (galactic) BH

M. Dovciak - Czech A.S.

- Accreting NS & WD

J. Poutanen - Univ. Turku

- Magnetars

R. Turolla - Univ Padova

- RQ AGN & Sgr A*

F. Marin - Obs. Strasbourg

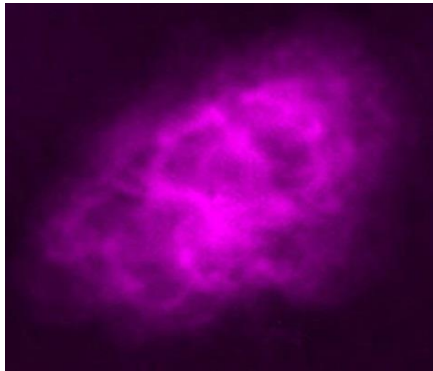
- Blazars and radiogalaxies

A. Marscher - Boston Univ.

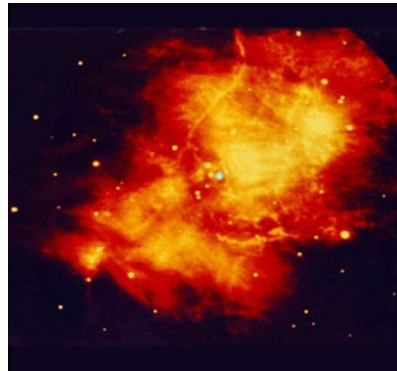


IXPE
Imaging
X-Ray
Polarimetry
Explorer

THE CRAB NEBULA OR THE IMPORTANCE OF IMAGING X-RAY POLARIMETRY



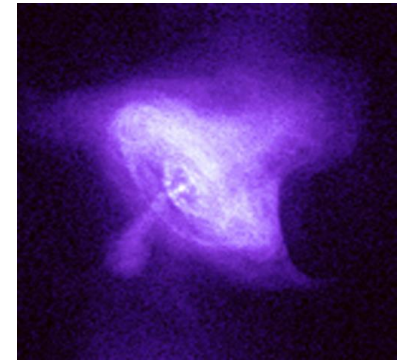
Radio (VLA)



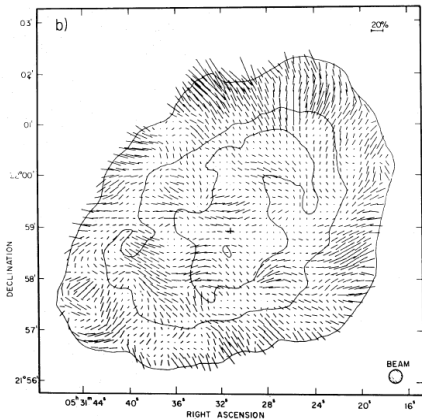
Infrared (Keck)



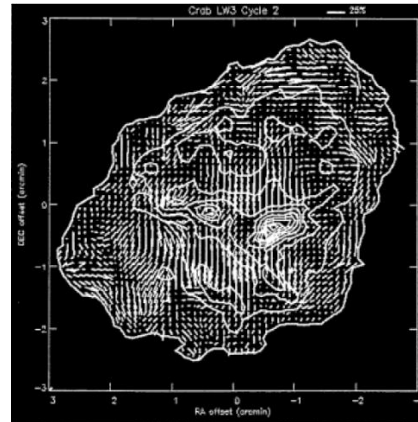
Optical (Palomar)



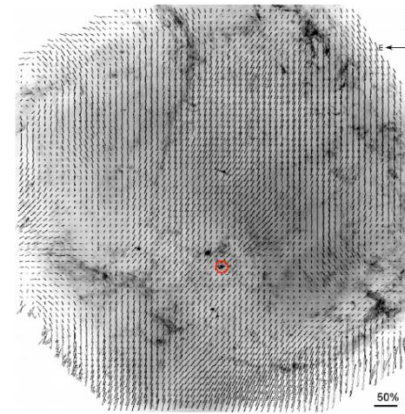
X-rays (Chandra)



Radio polarisation



IR polarisation



Optical polarisation

?

P=19% integrated over the entire nebula (Weisskopf et al. 1978)

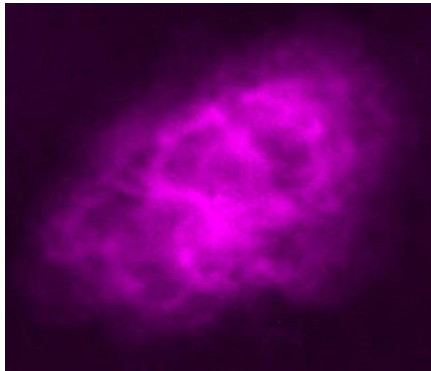
X-ray polarisation

X-rays probe **freshly accelerated** electrons and their acceleration site.

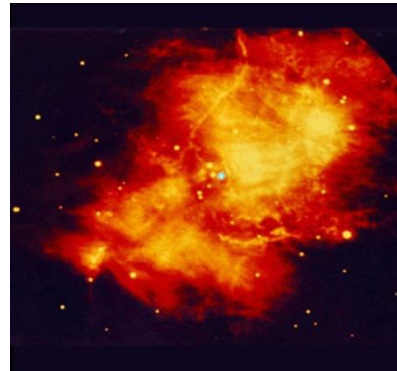


IXPE
Imaging
X-Ray
Polarimetry
Explorer

THE CRAB NEBULA OR THE IMPORTANCE OF IMAGING X-RAY POLARIMETRY



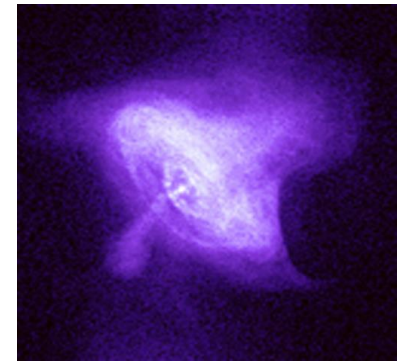
Radio (VLA)



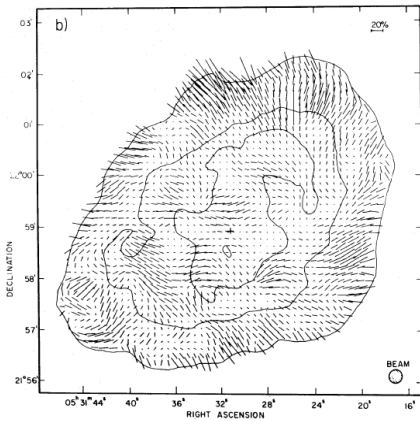
Infrared (Keck)



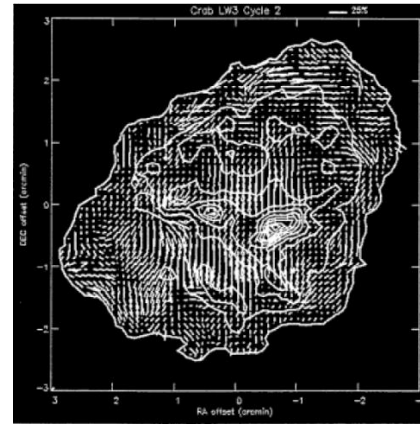
Optical (Palomar)



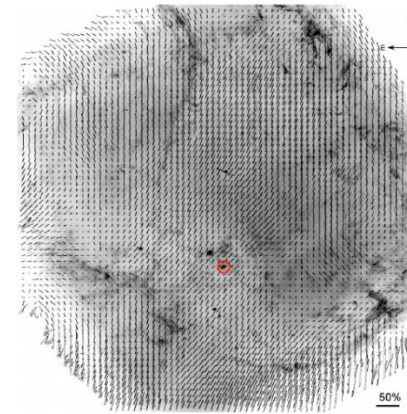
X-rays (Chandra)



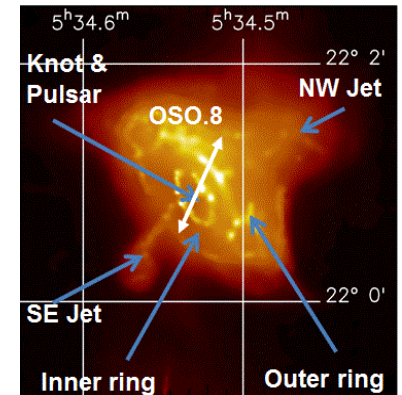
Radio polarisation



IR polarisation



Optical polarisation



X-ray polarisation

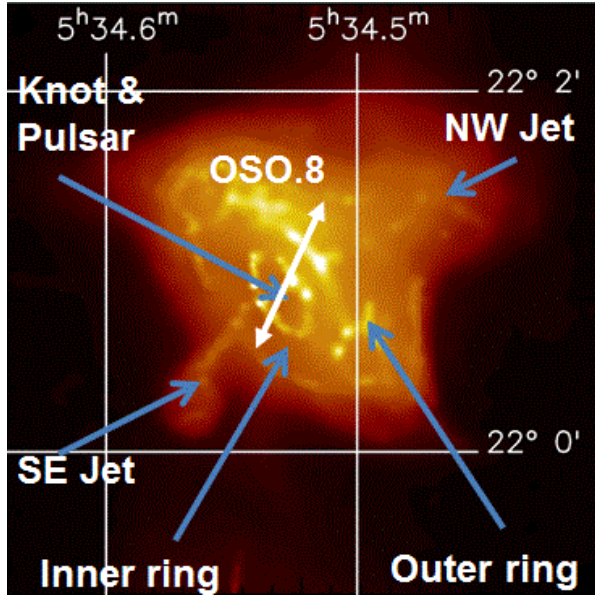
X-rays probe **freshly accelerated** electrons and their acceleration site.



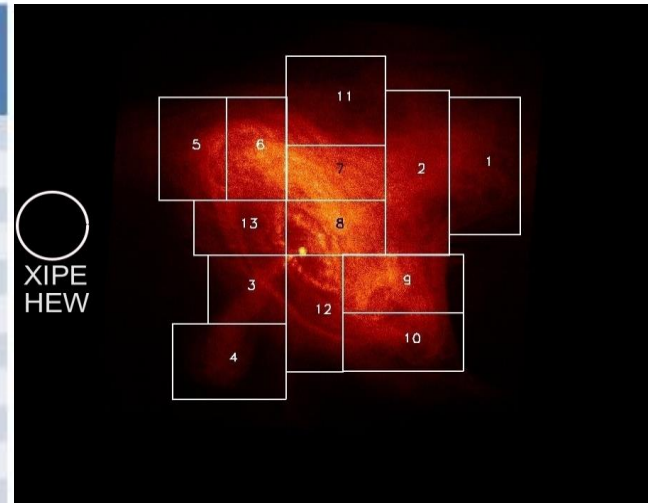
IXPE

Imaging
X-Ray
Polarimetry
Explorer

THE CRAB NEBULA OR THE IMPORTANCE OF IMAGING X-RAY POLARIMETRY



Region	σ degree (%)	σ angle (deg)	MDP (%)
1	± 0.60	± 0.96	1.90
2	± 0.41	± 0.65	1.30
3	± 0.68	± 1.10	2.17
4	± 0.86	± 1.39	2.76
5	± 0.61	± 0.97	1.93
6	± 0.46	± 0.75	1.48
7	± 0.44	± 0.70	1.40
8	± 0.44	± 0.71	1.41
9	± 0.46	± 0.74	1.47
10	± 0.60	± 0.97	1.92
11	± 0.52	± 0.83	1.65
12	± 0.53	± 0.85	1.69
13	± 0.59	± 0.95	1.89



40 ks with IXPE

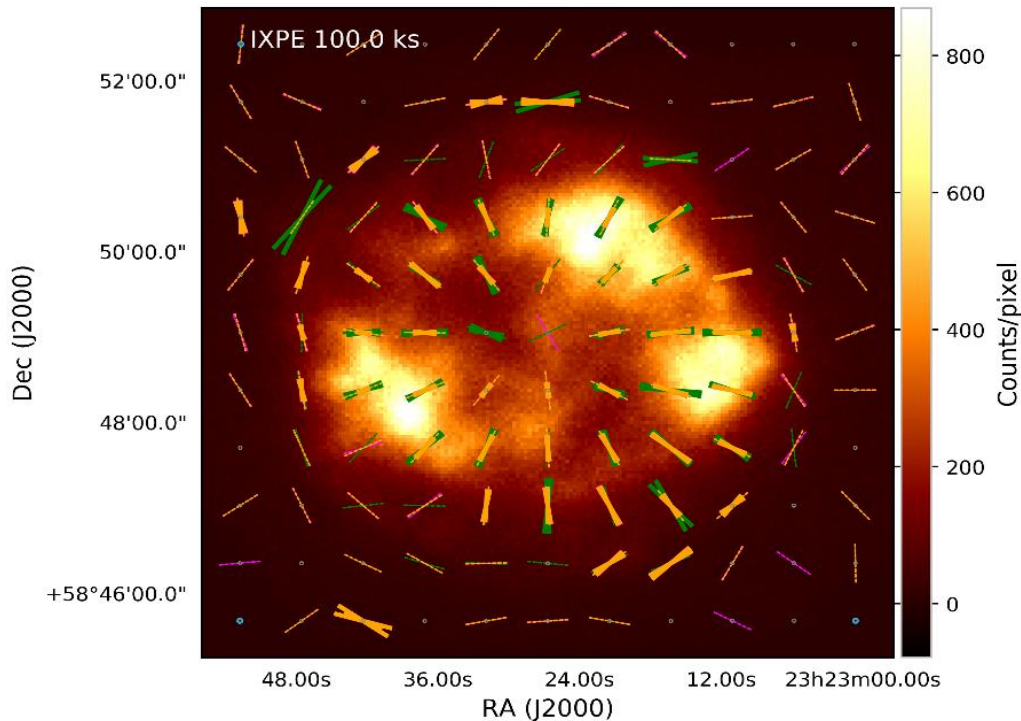
- The OSO-8 observation, integrated over the entire nebula, measured a position angle that is tilted with respect to the jets and torus axes.
- What is the role of the magnetic field (turbulent or not?) in accelerating particles and forming structures?
- IXPE imaging capabilities will allow us to measure the pulsar polarisation by separating it from the much brighter nebula emission.
- Other PWN, up to 5 or 6, are accessible for larger exposure times (e.g. Vela or the “Hand of God”).

SUPERNOVA REMNANTS

Map of the magnetic field

Spectral imaging allows to separate the thermalised plasma from the regions where shocks accelerate particles.

What is the orientation of the magnetic field? How ordered is it? The spectrum cannot tell...



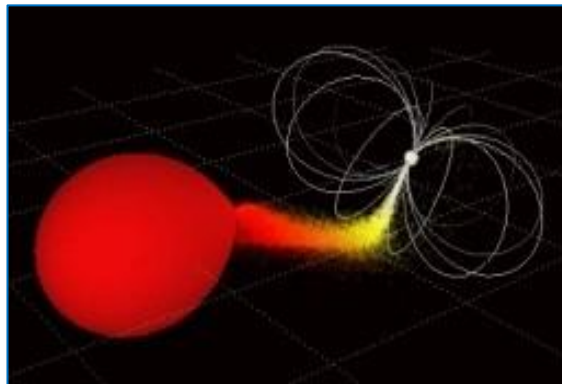
**100 ks IXPE observation
of Cas A**

**credit: Kandel, Rodriguez
& Romani**

MAGNETIZED COMPACT OBJECTS

The study of highly magnetized sources such as white dwarfs and neutron stars is definitely one of the most exciting science cases for a X-ray polarimeter.

Magnetic Cataclysmic
Variables and Novae



NSs accreting matter from a
companion star
(millisecond pulsars,
accreting X-ray pulsars)



Isolated NSs
(rotation powered pulsars, magnetars)



B-field

$10^7 \div 10^8$ G

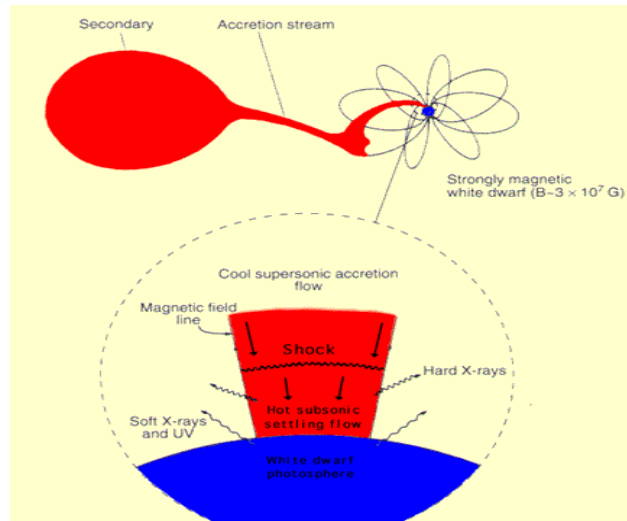
$10^8 \div 10^9$ G

10^{12} G

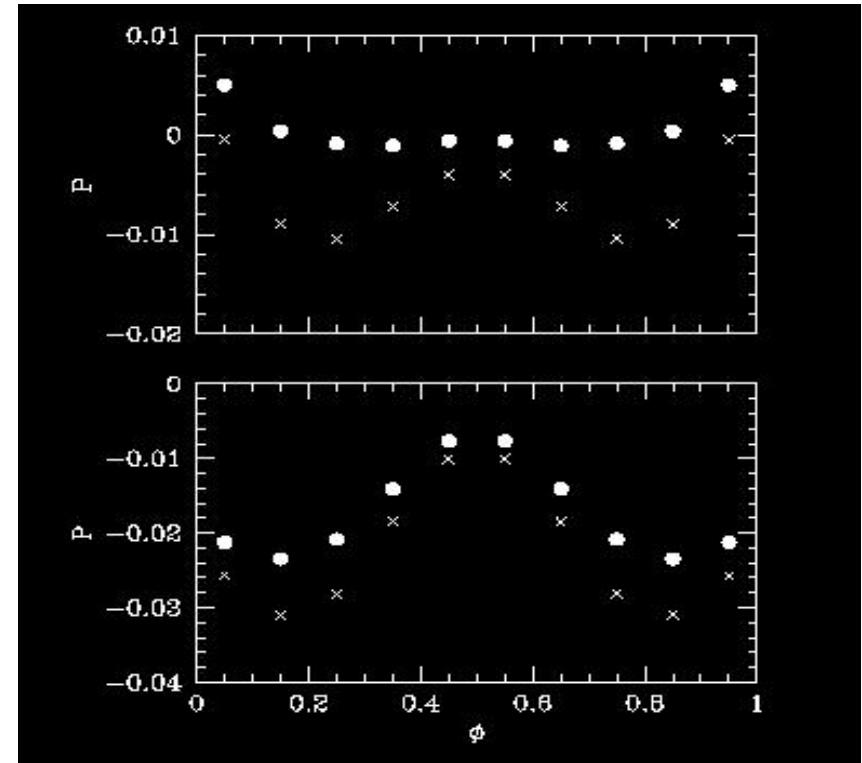
$10^{12} \div 10^{13}$ G

$10^{14} \div 10^{15}$ G

ACCRETING WHITE DWARFS



Accretion in Magnetic Cataclysmic Variables occurs in accretion column, Main emission process is thermal bremsstrahlung, but scattering may be relevant. Polarization gives informations on the accretion mode (Matt 2004; McNamara et al, 2008)



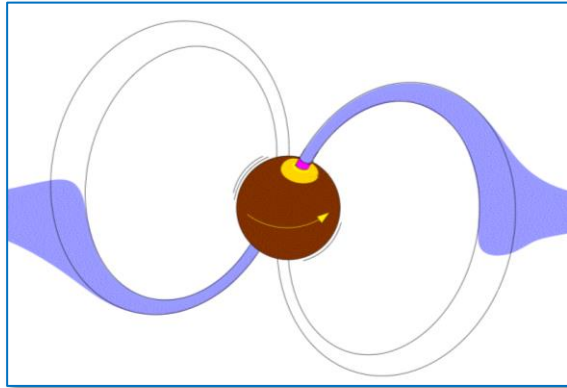
Matt 2004



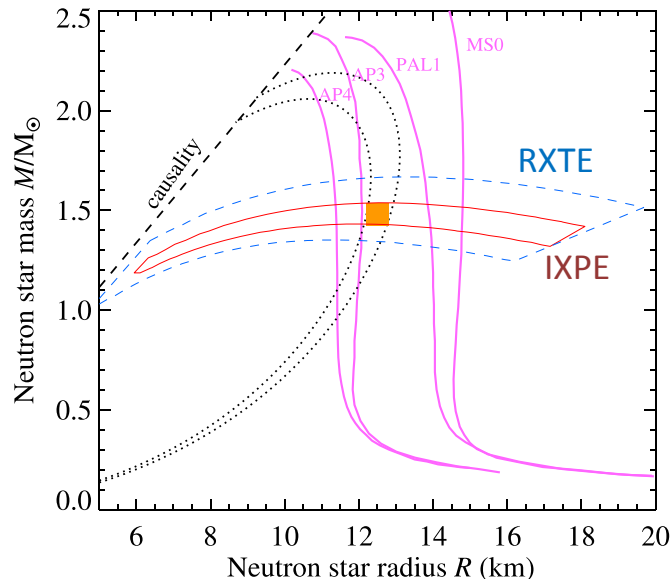
IXPE

Imaging
X-Ray
Polarimetry
Explorer

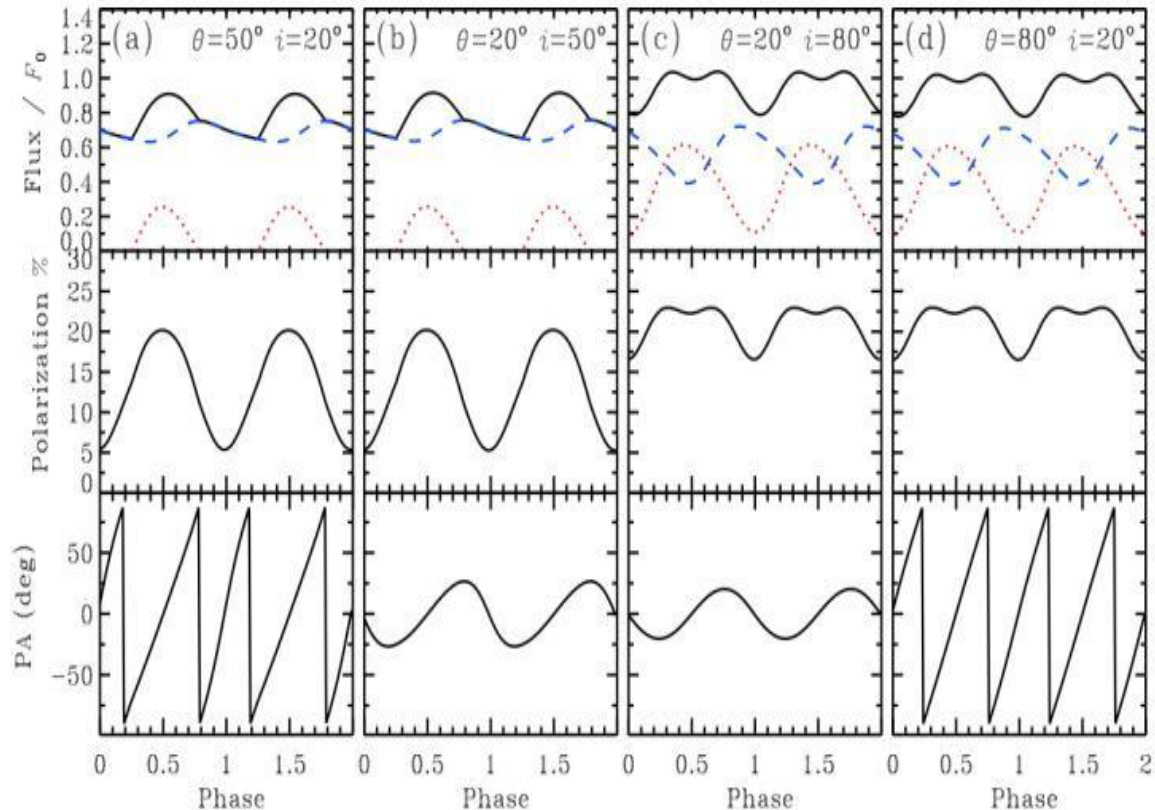
ACCRETING MILLISECOND PULSARS



Emission due to scattering in hot spots
⇒ Phase-dependent linear polarization



Viironen & Poutanen 2004



Polarization measurements constrain the geometrical parameters of the system. When combined with spectral and timing measurements from e.g. NICER and ATHENA, the EoS of the NS can be constrained

ACCRETING NEUTRON STARS

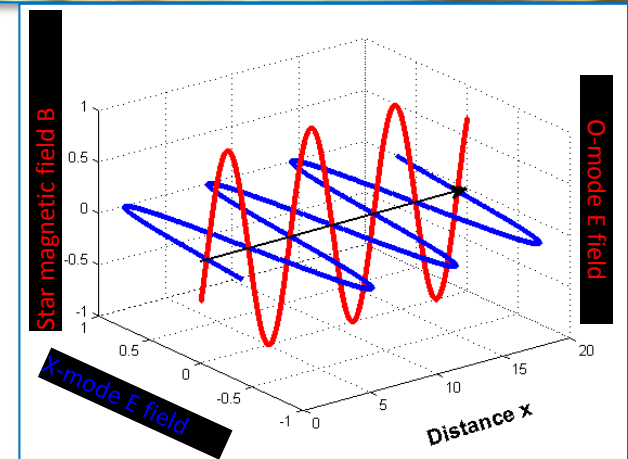
Opacity in highly magnetized plasma

$$\Rightarrow k_{\perp} \neq k_{\parallel}$$

Phase-dependent linear polarization

From the (phase-resolved) swing
of the polarisation angle :

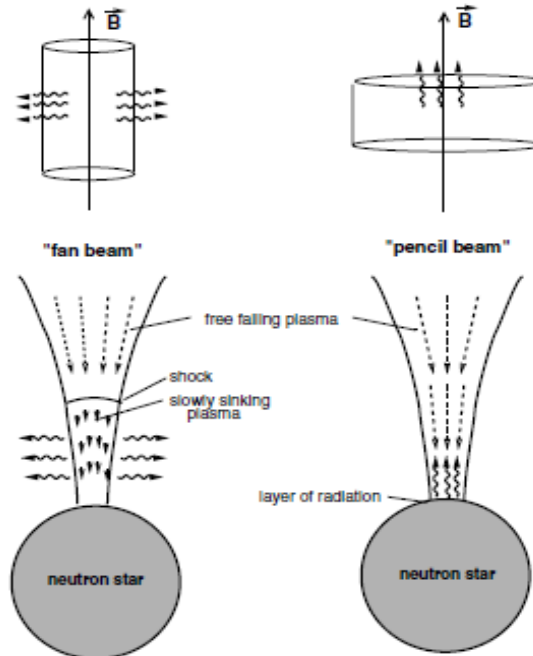
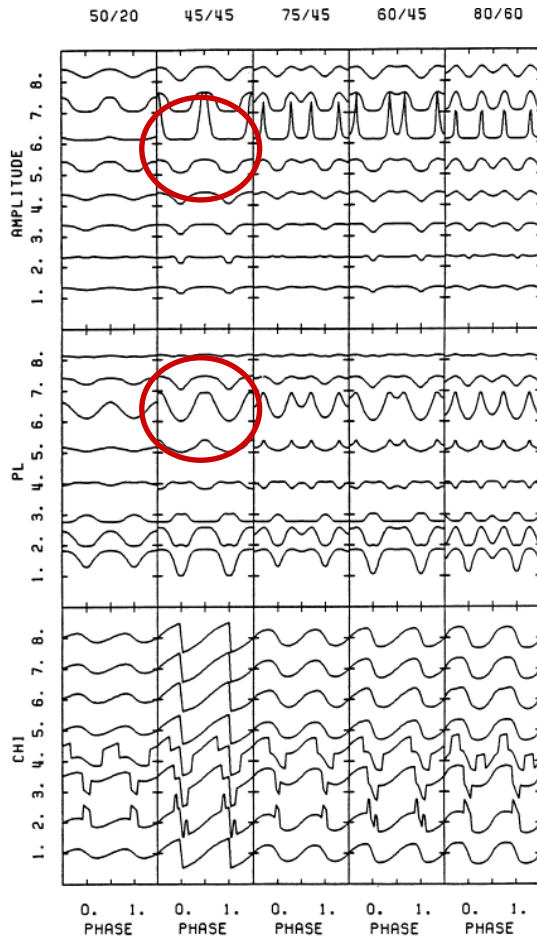
Orientation of the rotation axis
and inclination of the
magnetic field (required
for many purposes,
e.g. measure of
mass/radius



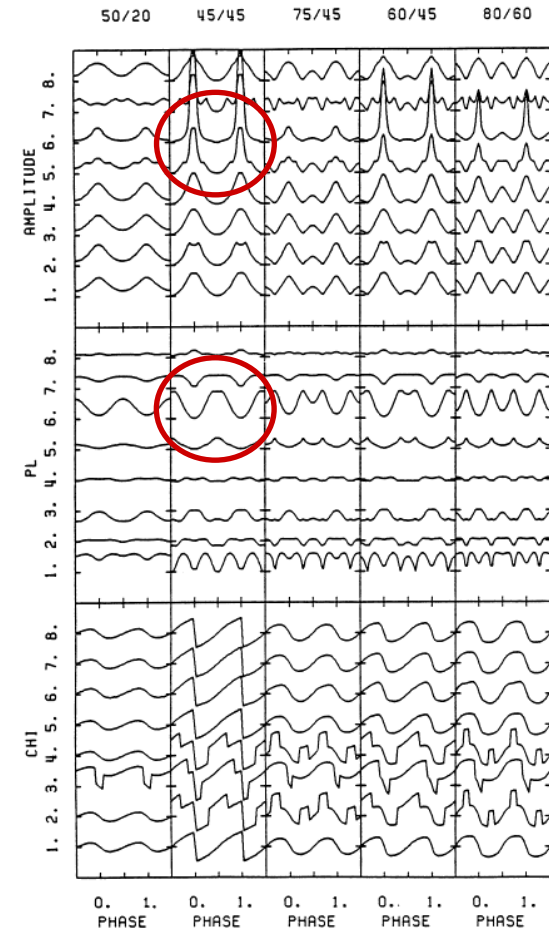
O-mode the E-field oscillates in the **k-B** plane
X-mode: the E-field oscillates perp. to the **k-B** plane

ACCRETING NEUTRON STARS

“Fan” vs. “Pencil” beam



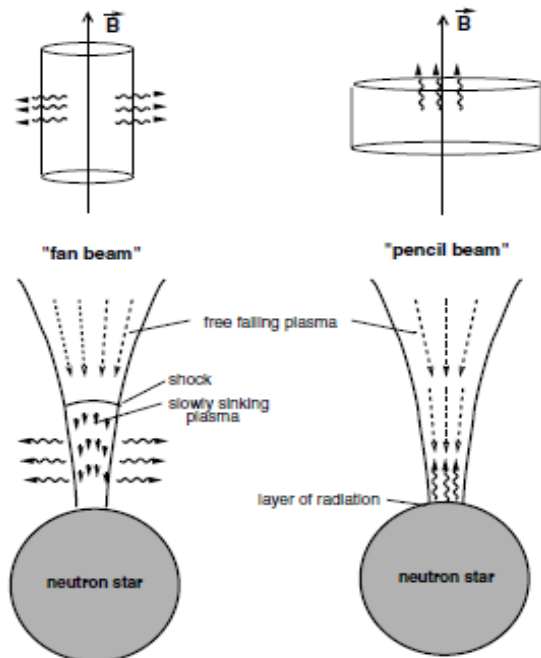
Meszaros et al. 1988



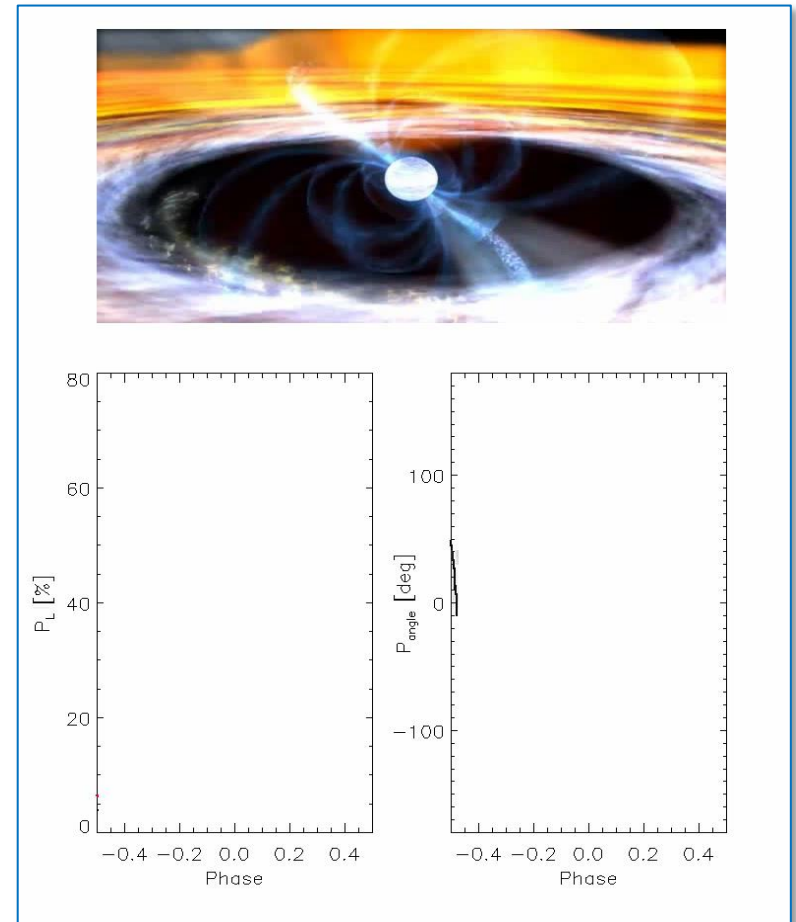
ACCRETING NEUTRON STARS

Credit: V. Doroshenko

“Fan” vs. “Pencil” beam



Meszaros et al. 1988



QED EFFECTS IN MAGNETARS

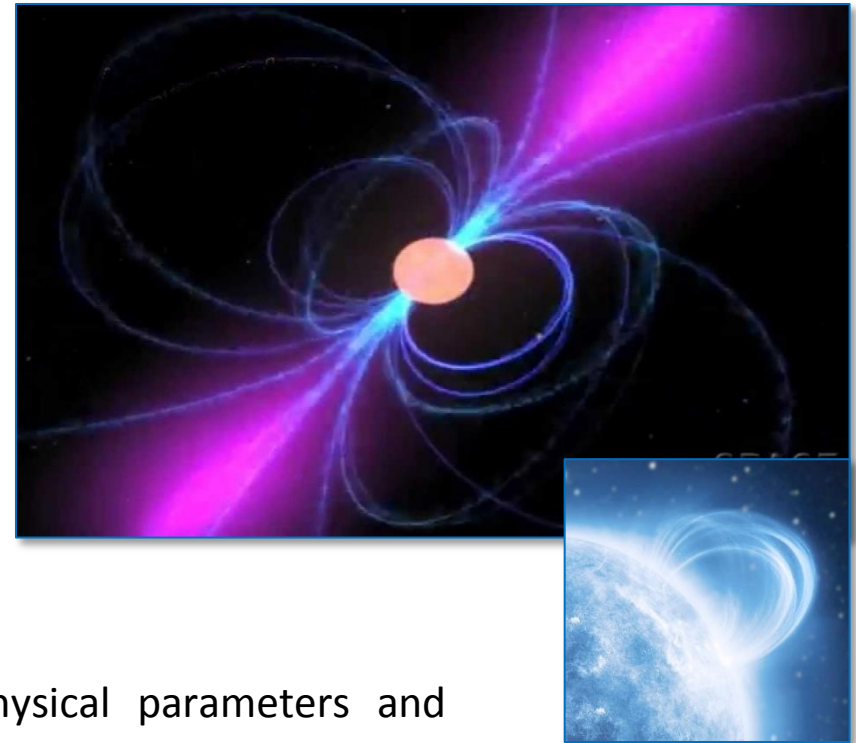
Magnetars are isolated neutron stars powered by huge magnetic fields ($B \sim 10^{14} - 10^{15}$ G, $B_{\text{qed}} \approx 4.4 \times 10^{13}$ G).

High X-ray activity (bursts, flares)
→ rapid magnetic field reconfiguration

Instability may develop in the core, crust, magnetosphere (reconnection)
→ highly twisted, non dipolar magnetic field

X-ray emission highly polarized

Spectral analysis alone can not disambiguate physical parameters and pinpoint the source geometry



Polarimetry can:

- Map the magnetic field
- Probe the magnetosphere physical parameters
- Probe “vacuum birefringence”



IXPE

Imaging
X-Ray
Polarimetry
Explorer

QED EFFECTS IN MAGNETARS

Folgerungen aus der Diracschen Theorie des Positrons.

Von **W. Heisenberg** und **H. Euler** in Leipzig.

Mit 2 Abbildungen. (Eingegangen am 22. Dezember 1935.)

Aus der Diracschen Theorie des Positrons folgt, da jedes elektromagnetische Feld zur Paarerzeugung neigt, eine Abänderung der Maxwell'schen Gleichungen des Vakuums. Diese Abänderungen werden für den speziellen Fall berechnet, in dem keine wirklichen Elektronen und Positronen vorhanden sind, und in dem sich das Feld auf Strecken der Compton-Wellenlänge nur wenig ändert. Es ergibt sich für das Feld eine Lagrange-Funktion:

PHYSICAL REVIEW

VOLUME 82, NUMBER 5

JUNE 1, 1951

On Gauge Invariance and Vacuum Polarization

JULIAN SCHWINGER

Harvard University, Cambridge, Massachusetts

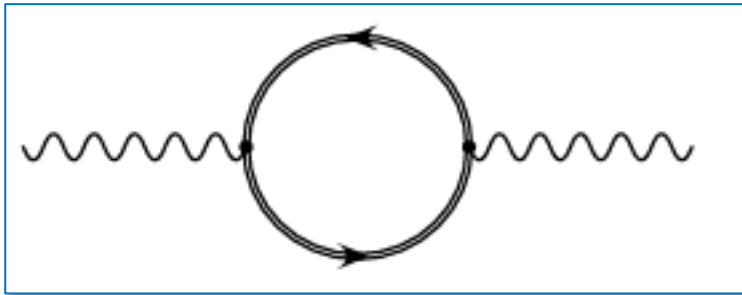
(Received December 22, 1950)

This paper is based on the elementary remark that the extraction of gauge invariant results from a formally gauge invariant theory is ensured if one employs methods of solution that involve only gauge covariant quantities. We illustrate this statement in connection with the problem of vacuum polarization by a prescribed electromagnetic field. The vacuum current of a charged Dirac field, which can be expressed in terms of the Green's function of that field, implies an addition to the action integral of the elec-

a spin zero neutral meson arising from the polarization of the proton vacuum. We obtain approximate, gauge invariant expressions for the effective interaction between the meson and the electromagnetic field, in which the nuclear coupling may be scalar, pseudoscalar, or pseudovector in nature. The direct verification of equivalence between the pseudoscalar and pseudovector interactions only requires a proper statement of the limiting processes involved. For arbitrarily varying fields, perturbation methods can

QED EFFECTS IN MAGNETARS

$$\mathcal{L} \simeq \frac{1}{2}(\mathbf{E}^2 - \mathbf{B}^2) + \frac{2\alpha_{\text{QED}}}{45} \frac{(\hbar/mc)^3}{mc^2} [(\mathbf{E}^2 - \mathbf{B}^2)^2 + 7(\mathbf{E} \cdot \mathbf{B})^2]$$



Expanding the action for a uniform field plus a small photon field:

$$\mathbf{E} = \mathbf{E}_0 + \delta\mathbf{E}, \quad \mathbf{B} = \mathbf{B}_0 + \delta\mathbf{B}$$

We obtain:

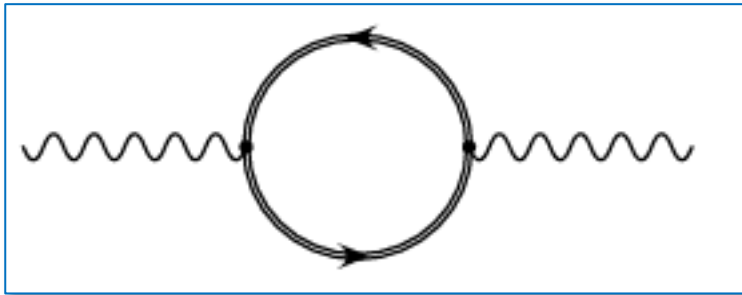
$$n_{\parallel} - n_{\perp} = \frac{\alpha_{\text{QED}}}{30\pi} \left(\frac{B}{B_{\text{QED}}} \right)^2 \sin^2 \theta$$

Where is θ the angle between the direction of propagation and the external field and

$$B_{\text{QED}} = \frac{m_e^2 c^3}{\hbar e} = 4.4 \times 10^{13} \text{ G}$$

QED EFFECTS IN MAGNETARS

$$\mathcal{L} \simeq \frac{1}{2}(\mathbf{E}^2 - \mathbf{B}^2) + \frac{2\alpha_{\text{QED}}}{45} \frac{(\hbar/mc)^3}{mc^2} [(\mathbf{E}^2 - \mathbf{B}^2)^2 + 7(\mathbf{E} \cdot \mathbf{B})^2]$$



Expanding the action for a uniform field plus a small photon field:

$$\mathbf{E} = \mathbf{E}_0 + \delta\mathbf{E}, \quad \mathbf{B} = \mathbf{B}_0 + \delta\mathbf{B}$$

We obtain:

$$n_{\parallel} - n_{\perp} = \frac{\alpha_{\text{QED}}}{30\pi} \left(\frac{B}{B_{\text{QED}}} \right)^2 \sin^2 \theta$$

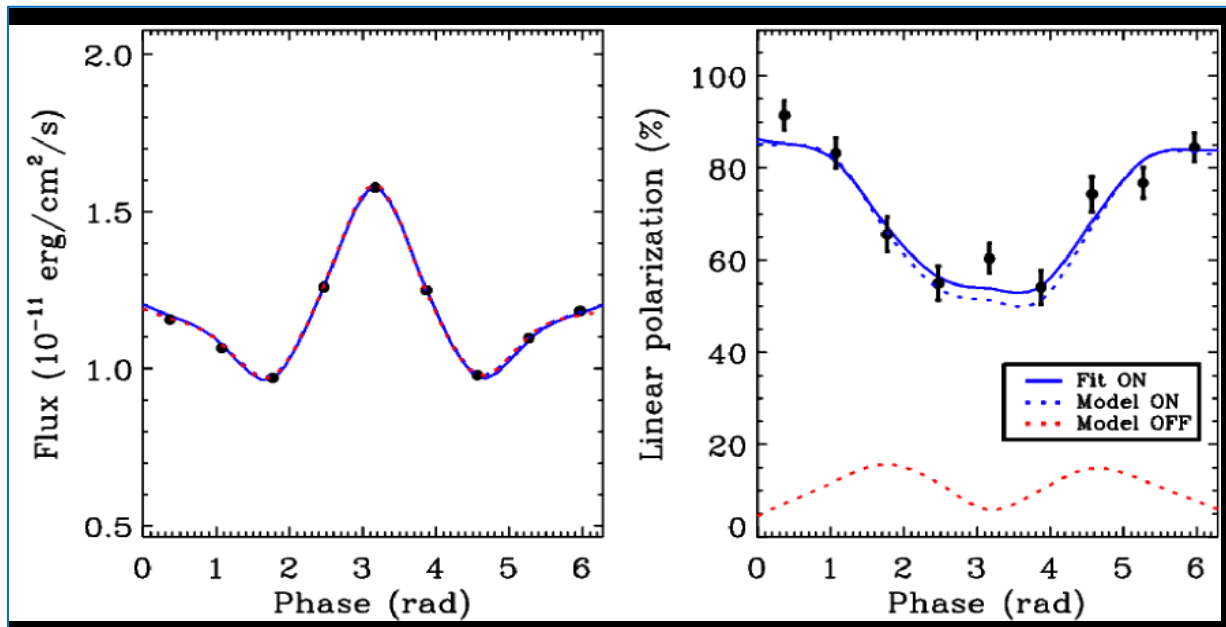
$$n_{\parallel} - n_{\perp} \approx 4 \times 10^{-24} \left(\frac{B}{1 \text{ T}} \right)^2$$

Very **small effect**
Hard to measure on
Earth

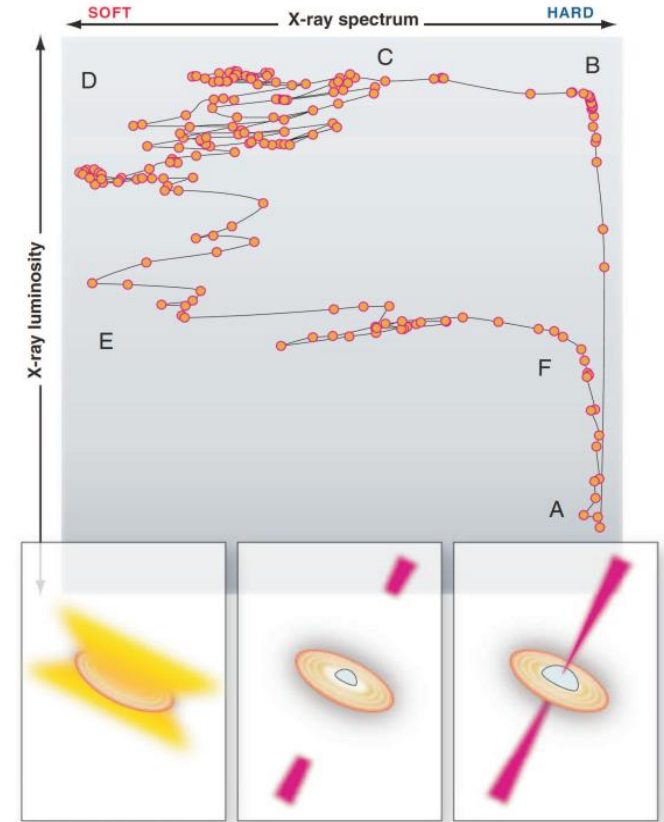
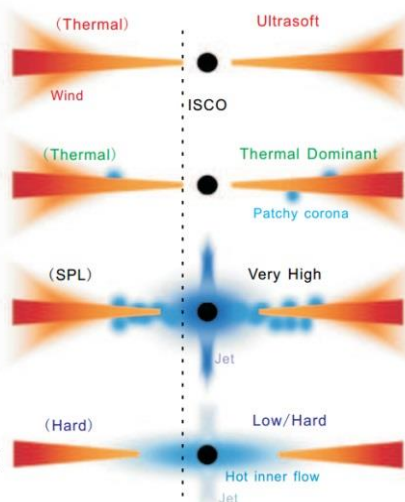
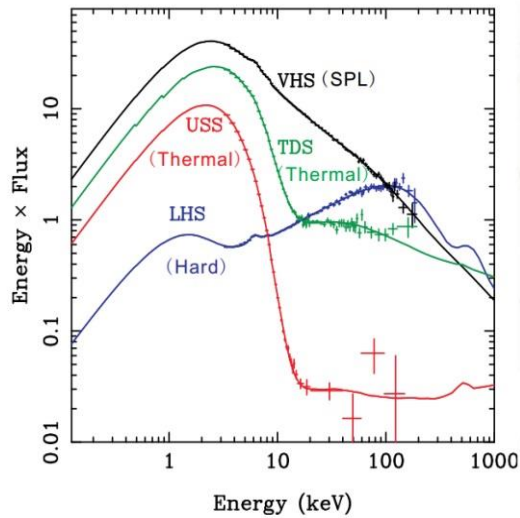
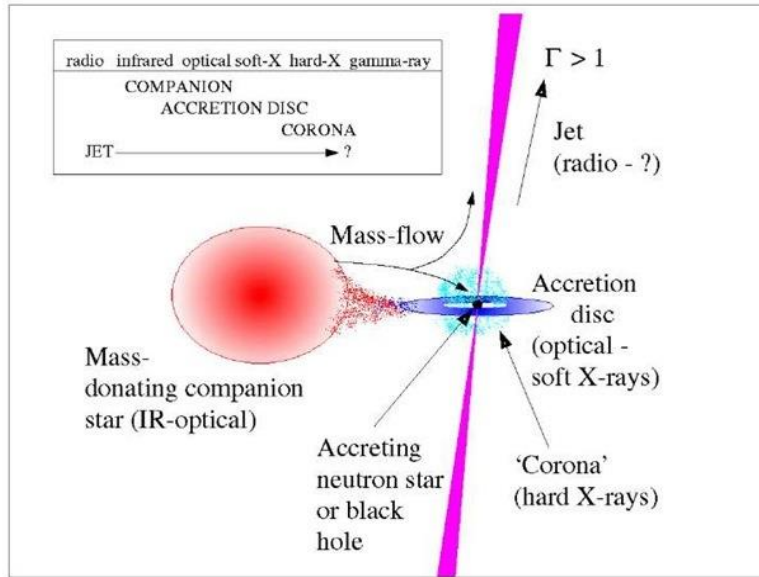
Effect is substantial in the vacuum near highly magnetized neutron stars

QED EFFECTS IN MAGNETARS

- **Magnetar is a neutron star with magnetic field up to 10^{15} G**
 - Billion times the strongest laboratory field
 - Non-linear QED predicts magnetized-vacuum birefringence
 - Can exclude QED-off at better than 99% c.l.

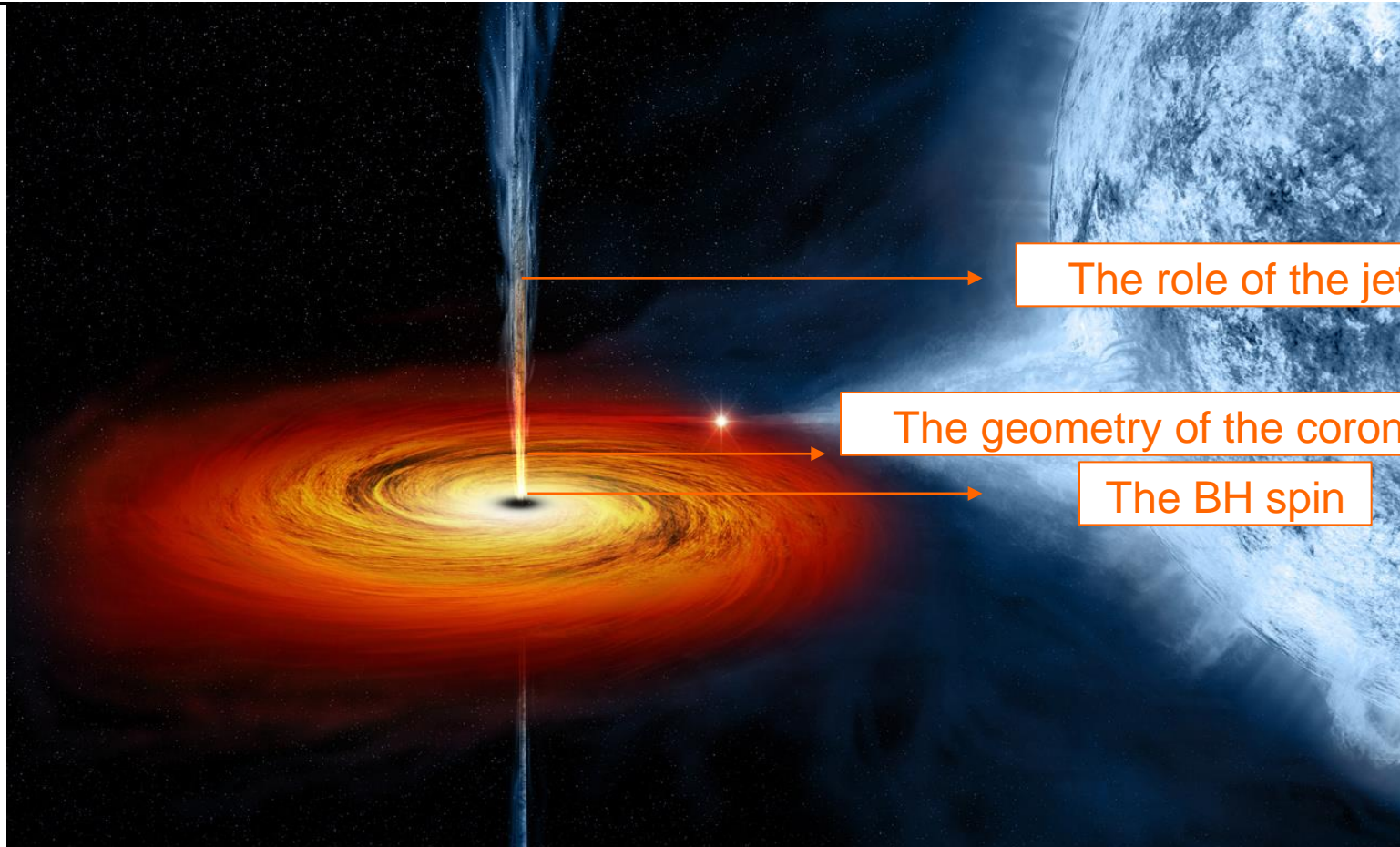


MICROQUASARS



Fender&Belloni 12

MICROQUASARS



The role of the jet

The geometry of the corona

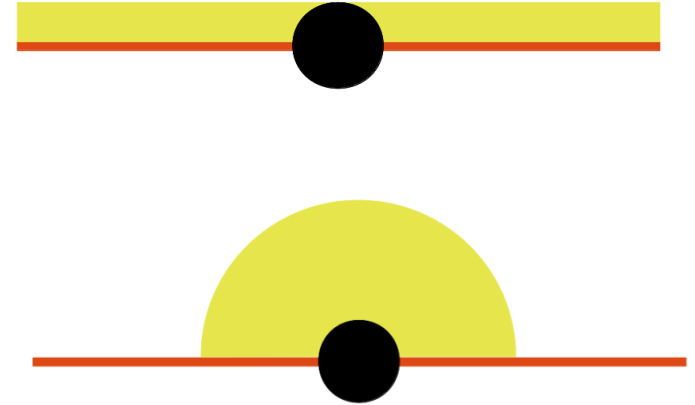
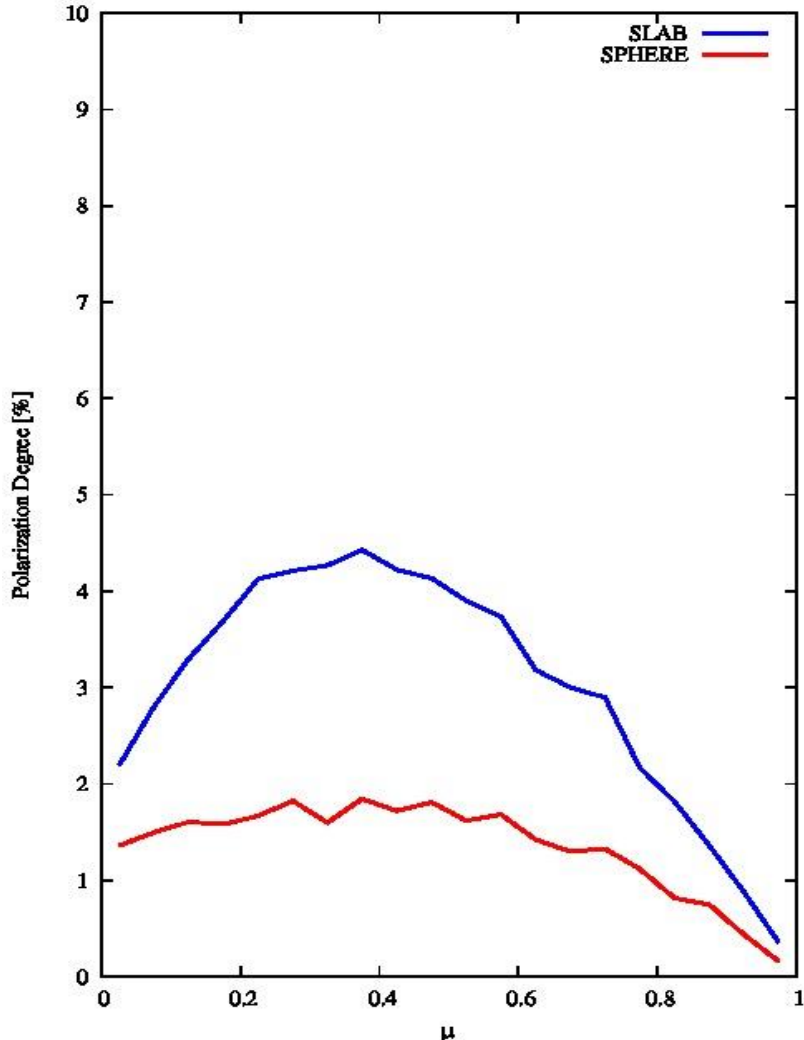
The BH spin

X-ray polarimetry can provide answers to several key problems:

The role of the jet - The geometry of the corona – The spin of the BH

MICROQUASARS: THE GEOMETRY OF THE HOT CORONA

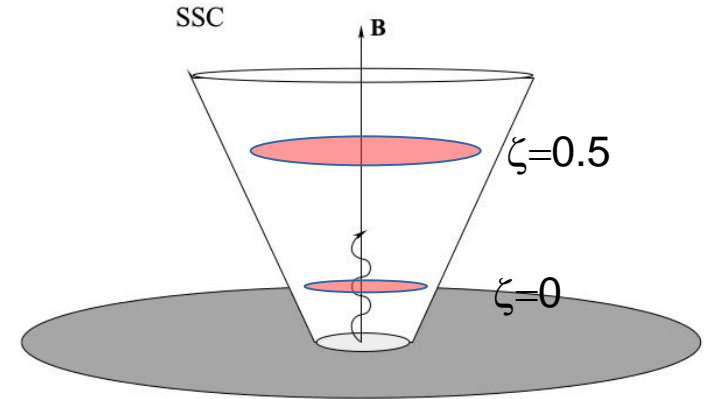
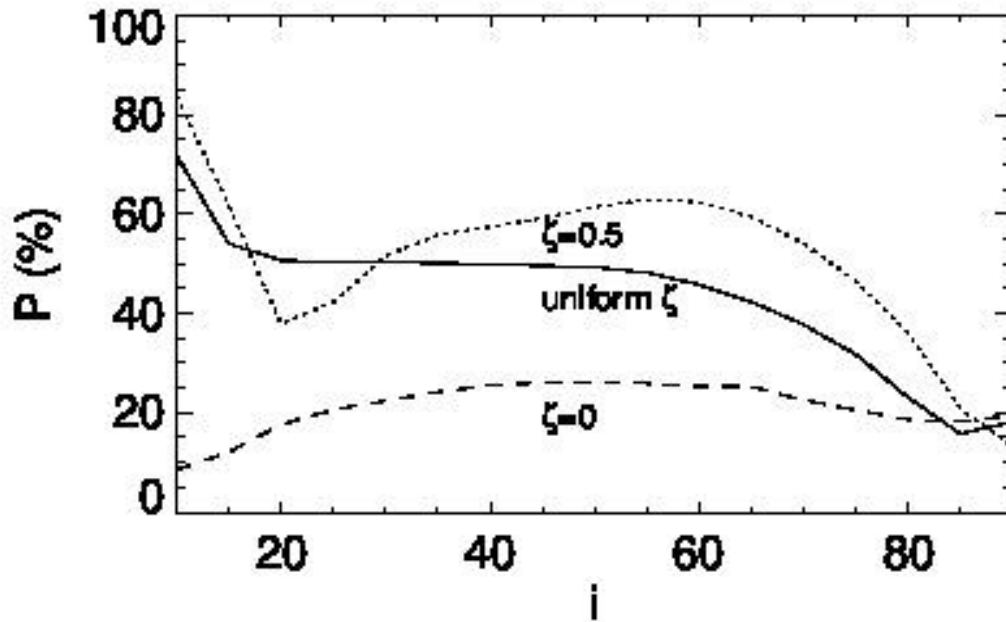
Pol Degree between 2-8 keV (6-500, mdot01, MBH10) tan1 kT100 - 20 bins



The geometry of the hot corona is unknown. Emission is expected to be polarized if the corona OR the radiation field are not spherical (Schnittman & Krolik 2010, Behestipour et al. 2017, Tamborra et al. 2018)

Courtesy: Francesco Tamborra

MICROQUASARS: THE ROLE OF THE JET



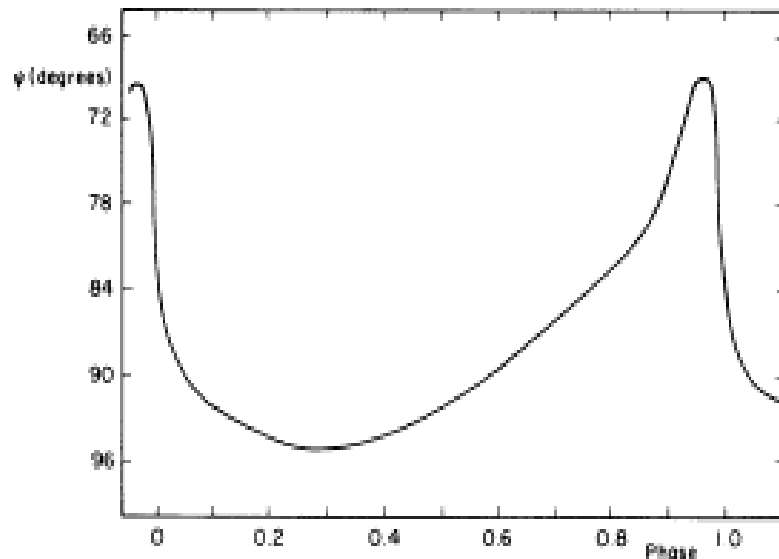
McNamara et al. 2009

Corona emission is predicted to be less than 10%.

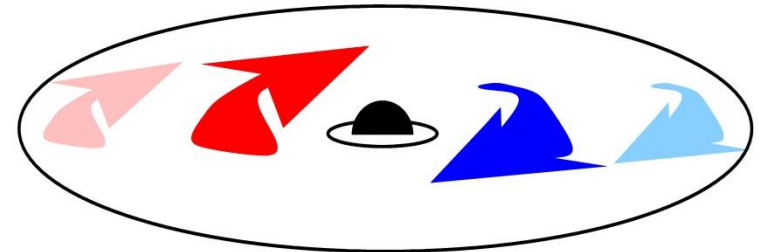
Much larger polarization degrees are expected for jet emission

MICROQUASARS: THE SPIN OF THE BLACK HOLE

- For an accreting Galactic BH in the soft state
 - Scattering polarizes the thermal disk emission
 - Polarization angle rotates due to GR effects
 - Polarization rotation is greatest for emission from inner disk
 - Inner disk is hotter, producing higher energy X-rays



Connors & Stark 1977



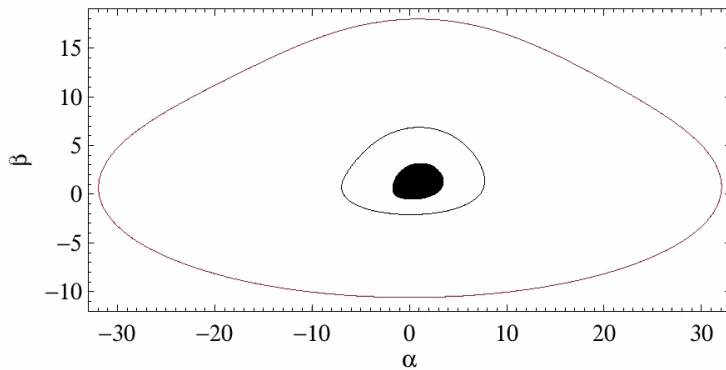
Orbiting spot with:
 $a=0.998$; $R=11.1 R_g$; $i=75.5$ deg

(Phase=0 when the spot is behind the BH)

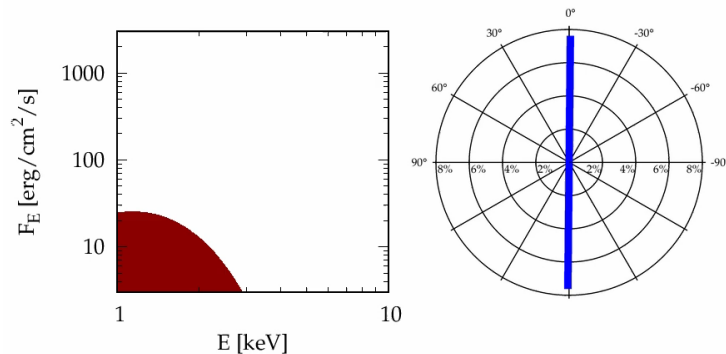
The PA of the net
 (i.e. phase-averaged) radiation is also rotated!

MICROQUASARS: THE SPIN OF THE BLACK HOLE

- For an accreting Galactic BH in the soft state
 - Scattering polarizes the thermal disk emission
 - Polarization angle rotates due to GR effects
 - Polarization rotation is greatest for emission from inner disk
 - Inner disk is hotter, producing higher energy X-rays



Rotation of the polarization angle with energy



Courtesy: Michal Dovciak



IXPE

Imaging
X-Ray
Polarimetry
Explorer

THE SPIN OF THE BLACK HOLE

- **For an accreting Galactic BH in the soft state**
 - Scattering polarizes the thermal disk emission
 - Polarization angle rotates due to GR effects
 - Polarization rotation is greatest for emission from inner disk
 - Inner disk is hotter, producing higher energy X-rays

Why another method, besides the three ones already in use?

Rotation of the polarization angle with energy

J1655-40:

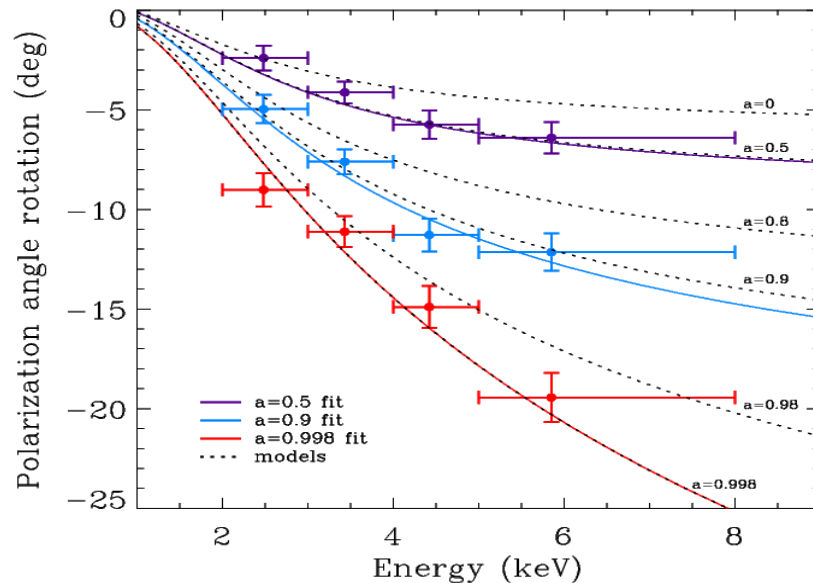
QPO $a = J/J_{\max} = 0.290 \pm 0.003$

Continuum: $a = J/J_{\max} = 0.7 \pm 0.1$

Iron line $a = J/J_{\max} = 0.95$

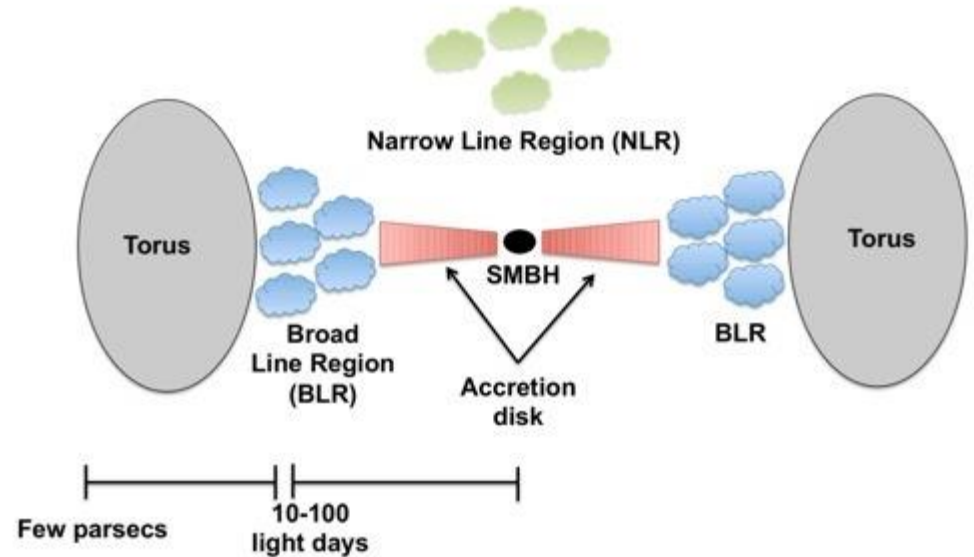
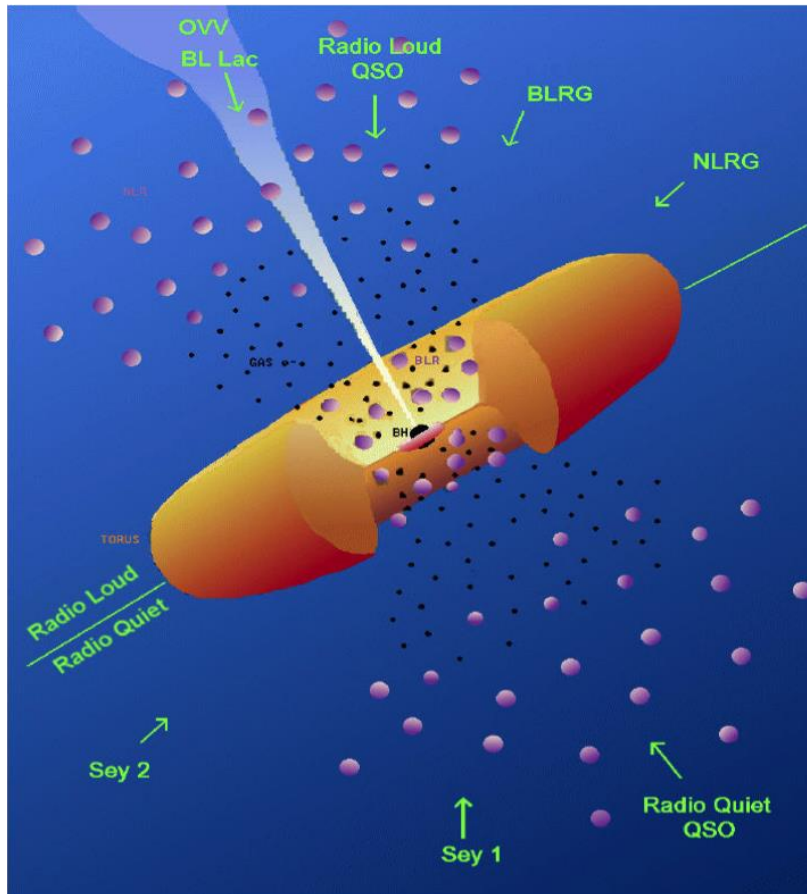
THE SPIN OF THE BLACK HOLE

- For an accreting Galactic BH in the soft state
 - Scattering polarizes the thermal disk emission
 - Polarization angle rotates due to GR effects
 - Polarization rotation is greatest for emission from inner disk
 - Inner disk is hotter, producing higher energy X-rays



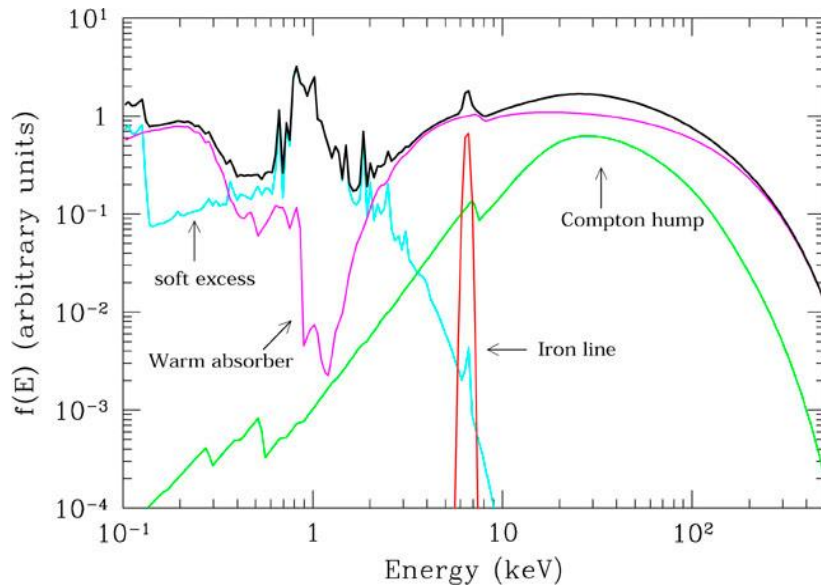
Rotation of the polarization angle with energy

ACTIVE GALACTIC NUCLEI

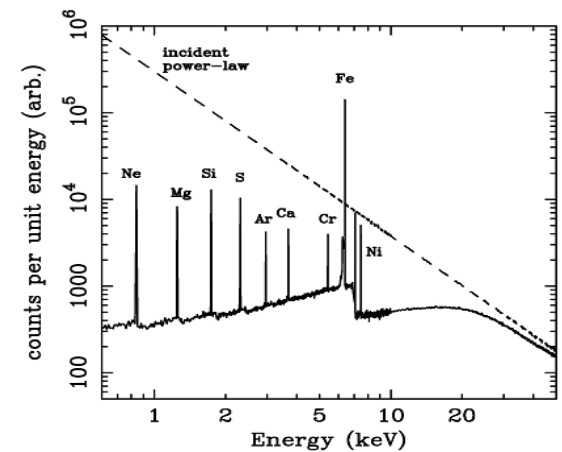
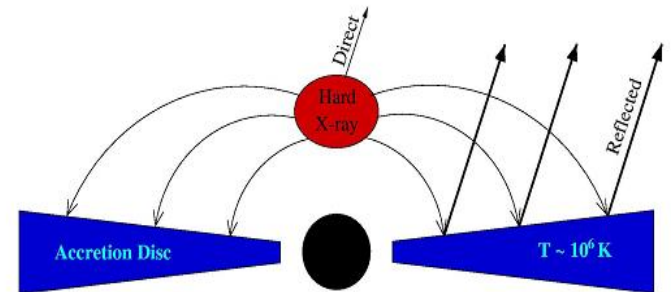


RADIO-QUIET ACTIVE GALACTIC NUCLEI

In AGN the primary X-ray emission is due to Inverse Compton by electrons in a hot corona of the UV/soft X-ray disc photons. It is likely to be significantly polarized (e.g. Haardt & Matt 1993, Poutanen & Vilhu 1993).

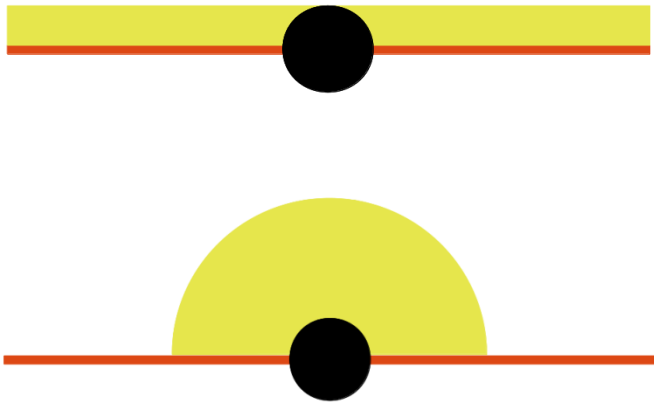


Part of the primary emission illuminates the disc and is reflected (and polarized) via Compton Scattering

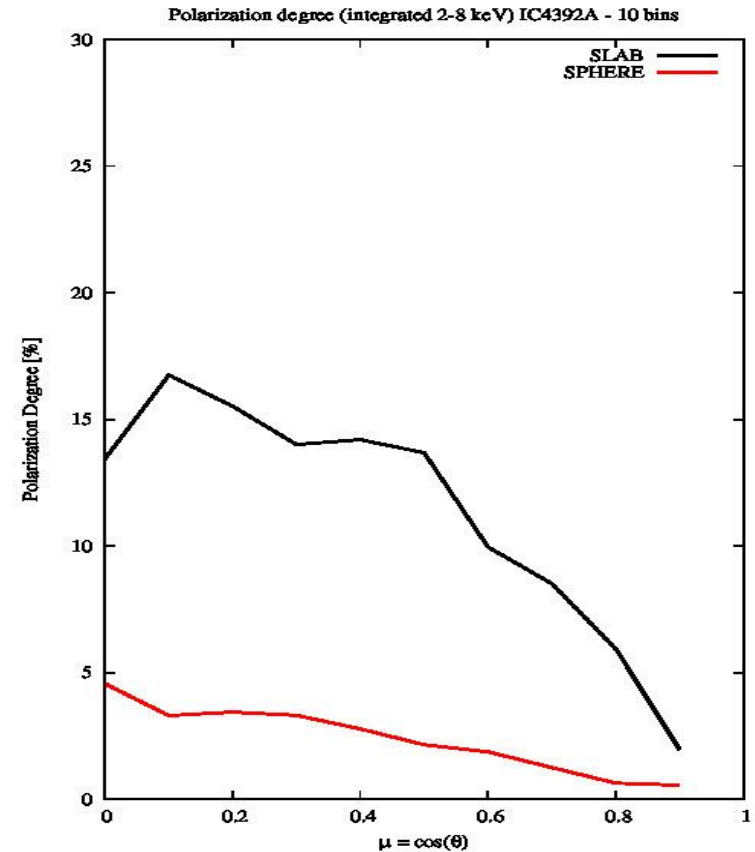


RQ AGN: THE HOT CORONA

The geometry of the hot corona is unknown.
Emission is expected to be polarized if the corona OR
the radiation field are not spherical
(Schnittman & Krolik 2010, Behestipour et al. 2017,
Tamborra et al. 2018)

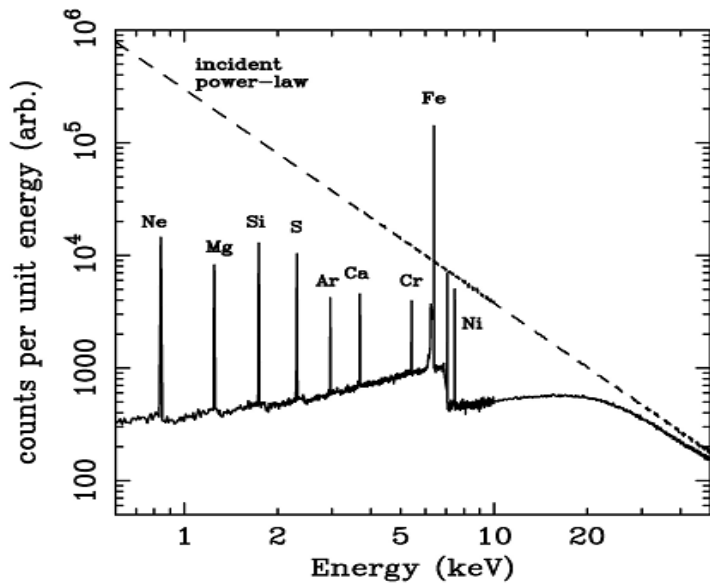


Example: polarization degree expected for IC 4329A
(Brenneman et al. 2014), calculated with the MoCA
Comptonization code (Tamborra et al. 2018).



Courtesy: Francesco Tamborra

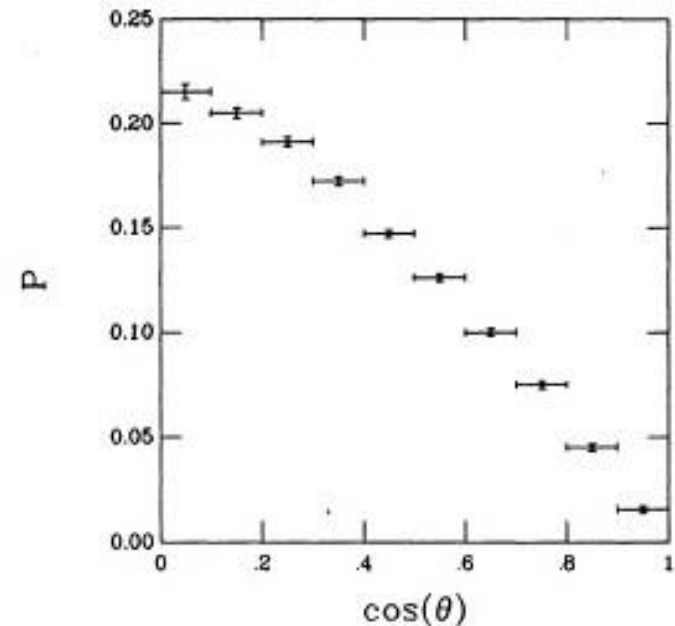
RQ AGN: THE SPIN OF THE BH



Reynolds et al. 1997

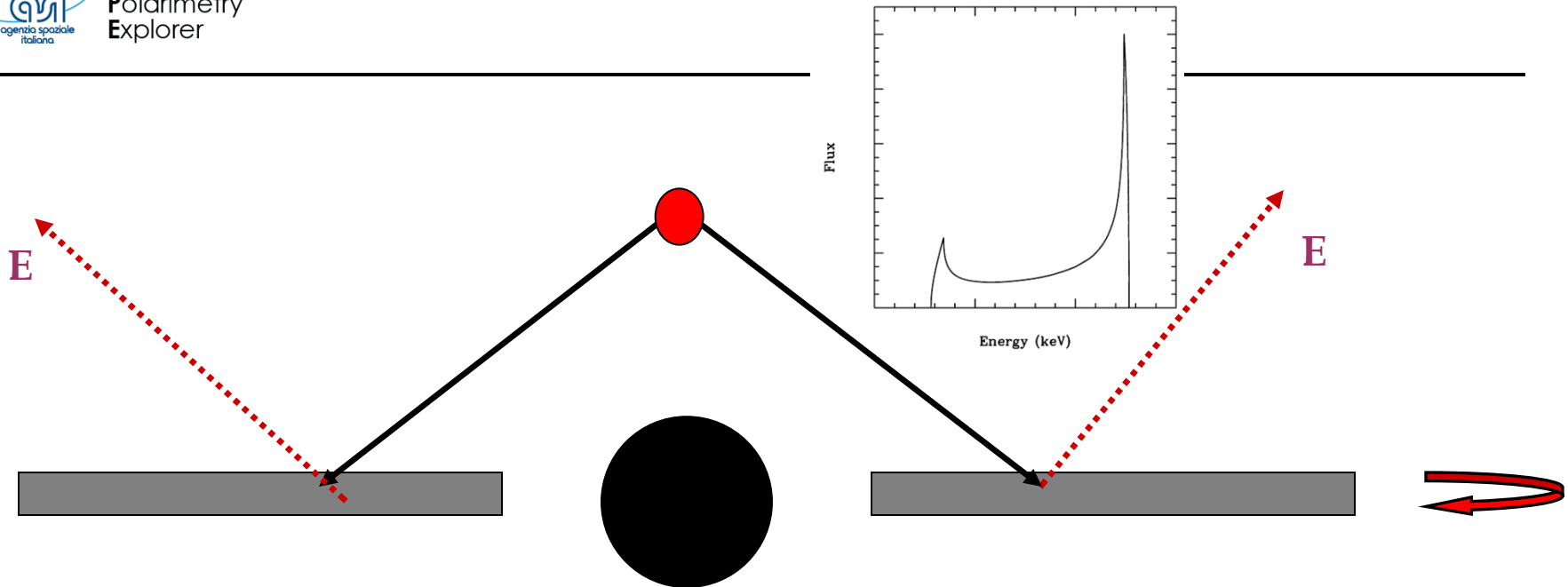
The exact values depend on the actual geometry of the system and on the polarization degree of the primary radiation.

Polarization of reflected (continuum) radiation is large, up to 20% (Matt et al. 1989) assuming isotropic illumination, a plane-parallel reflecting slab and unpolarized illuminating radiation.



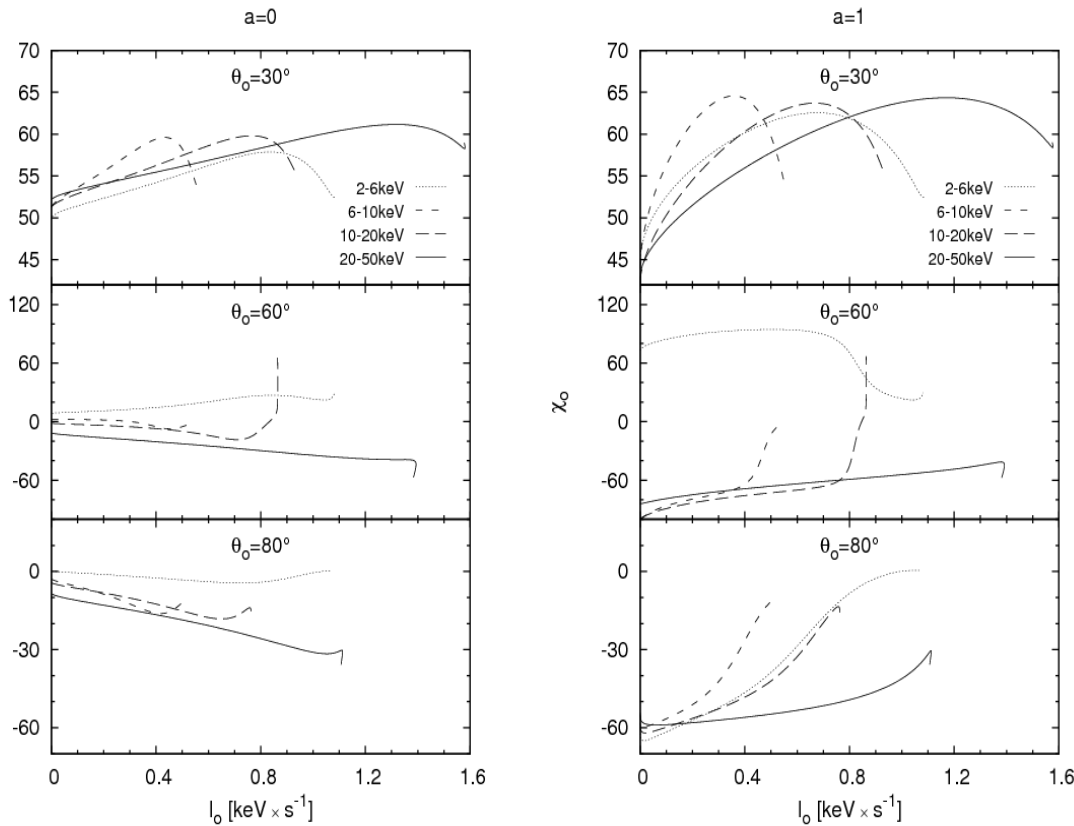
Matt et al. 1989

RQ AGN: THE SPIN OF THE BH



Breaking of the symmetry due to SR (Doppler boosting) also causes a rotation of the PA with respect to the Newtonian case. Changes in the illumination properties (e.g. in the height of the lamp-post) will cause changes in the total PA, which is therefore likely to be time- (and flux-) dependent. Variations of the height have been claimed in several AGN (e.g. Miniutti et al. 2003, Parker et al. 2014).

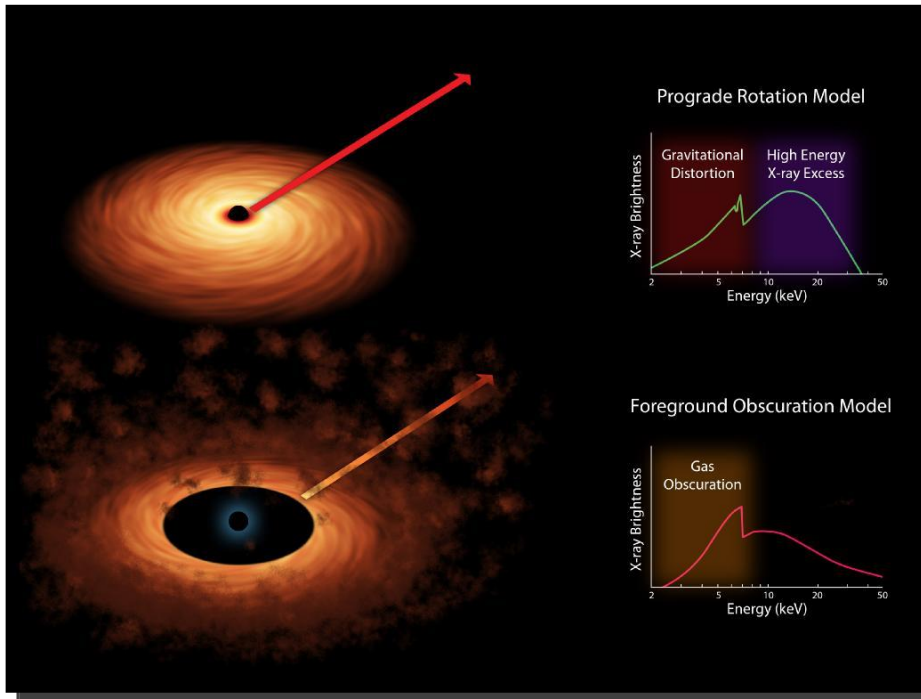
RQ AGN: THE SPIN OF THE BH



Variation of h with time implies a time and flux variation of the degree and angle of polarization.

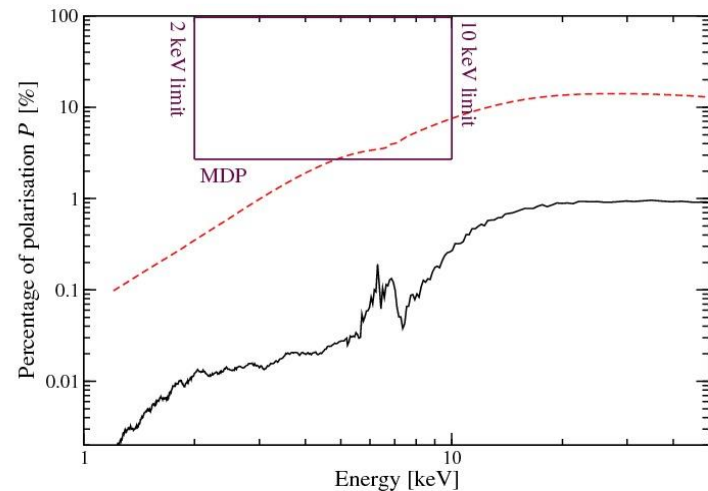
The effect depends also on the BH spin.

RQ AGN: REFLECTION OR ABSORPTION?



The relativistic reflection interpretation of the broad feature often seen in Seyfert galaxies has been challenged: complex absorption?

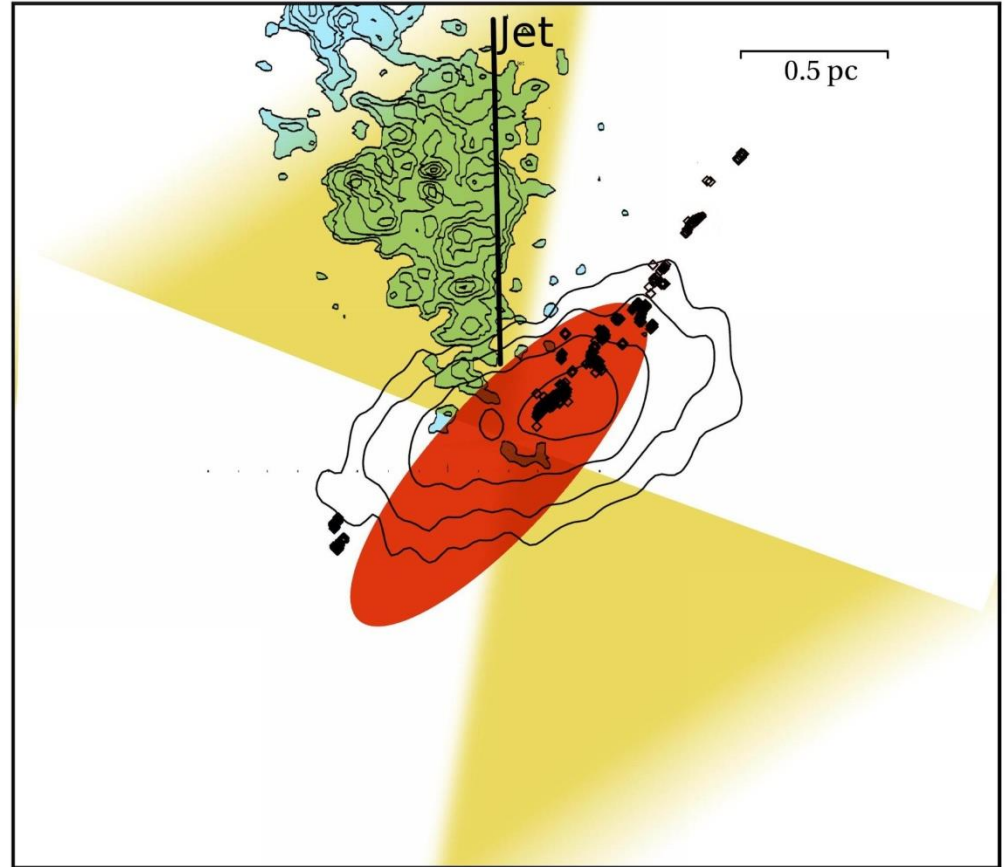
Polarimetry can distinguish between the two models



RQ AGN: ORIENTATION OF THE TORUS

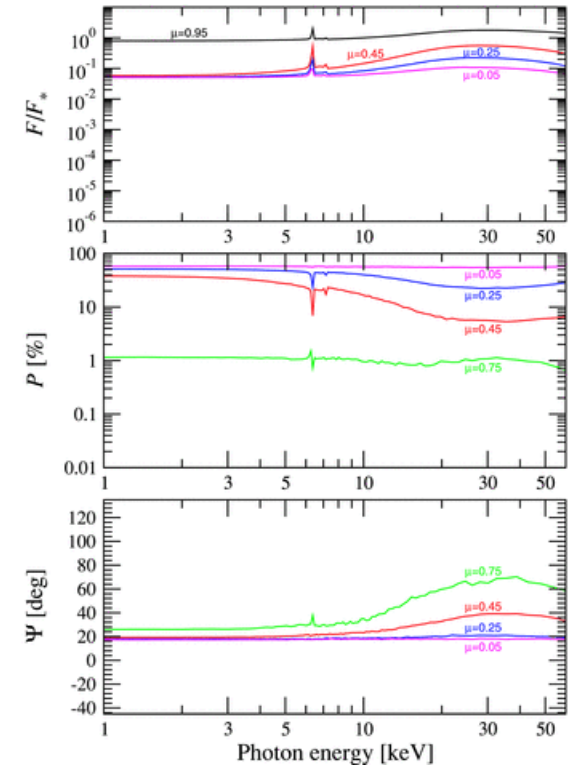
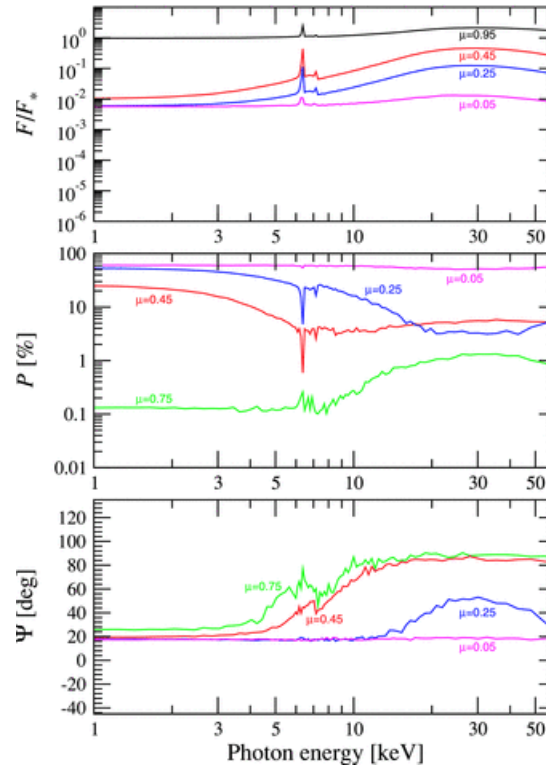
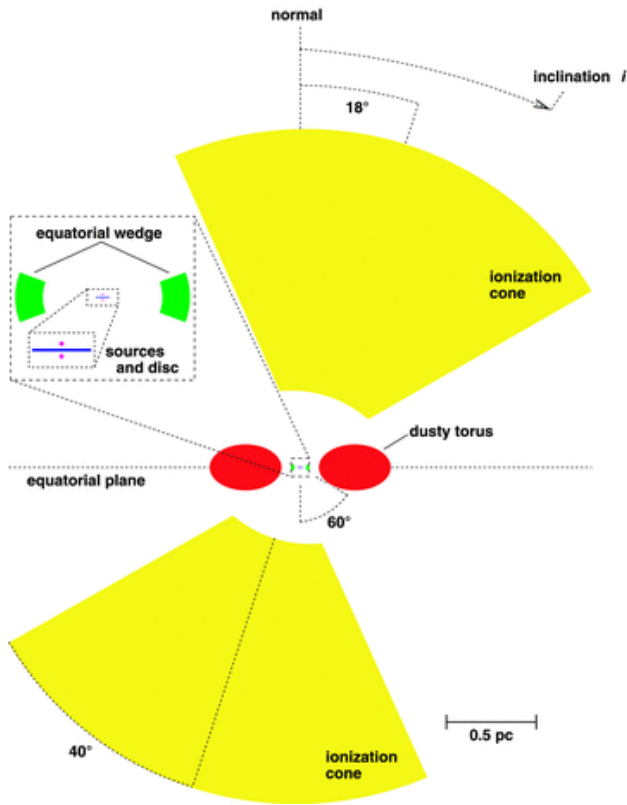
Geometry of the torus:

the polarization angle will give us the orientation of the torus, to be compared with IR results, and with the ionization cones (Goosmann & Matt 2011)



Raban et al. (2009)

RQ AGN: ORIENTATION OF THE TORUS

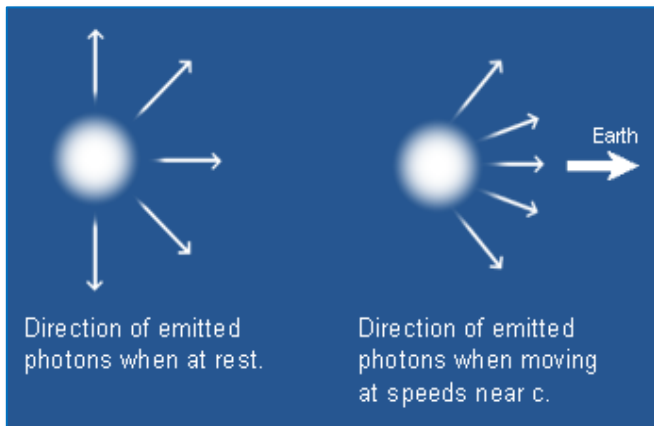


Goosmann & Matt (2011)

BLAZARS ...



Blazars are Active Galactic Nuclei with a jet directed towards us

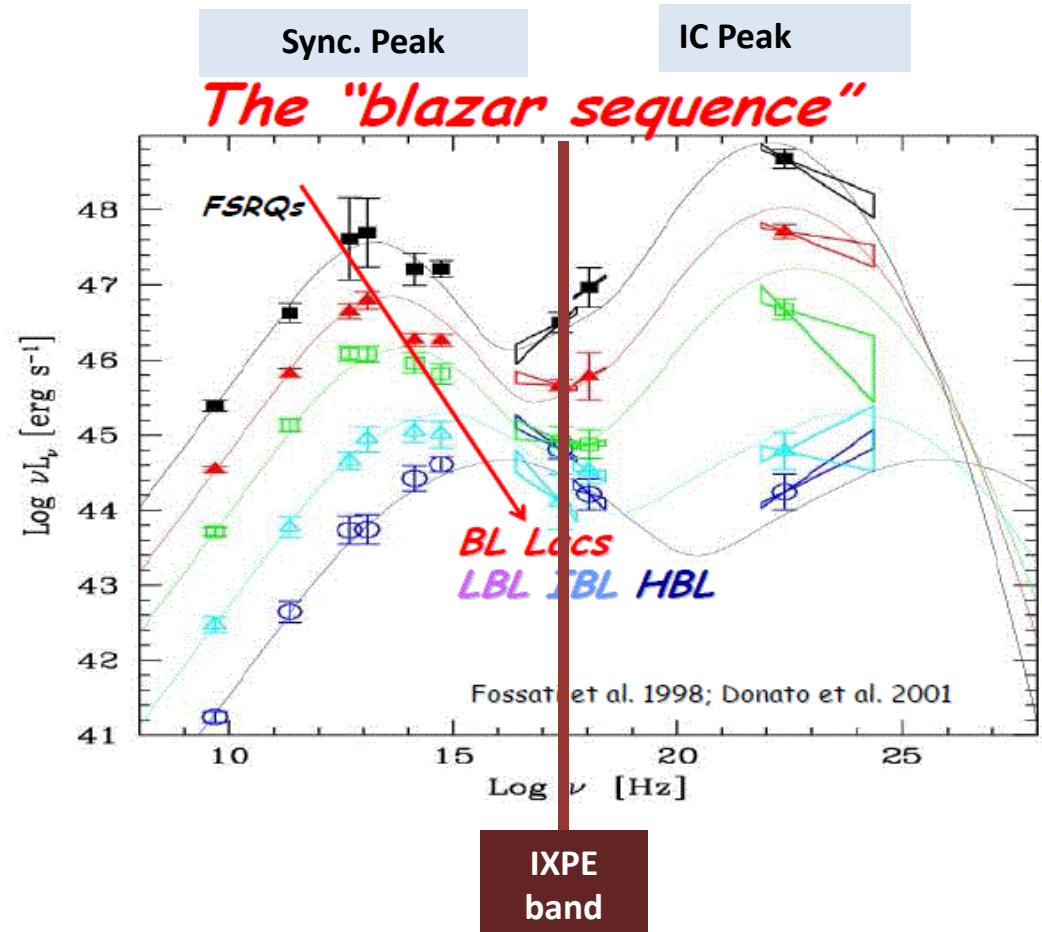


Due to a Special Relativity effect (aberration), the jet emission dominates over other emission components.

In **inverse Compton dominated** Blazars, multi- λ polarimetry observations can determine:

- **the composition of the jet** (hadronic vs. leptonic)
- **the origin of the seed photons** Synchrotron-Self Compton (SSC) \rightarrow The polarization angle is the same as for the synchrotron peak.

External Compton (EC) \rightarrow
The polarization angle may be different.



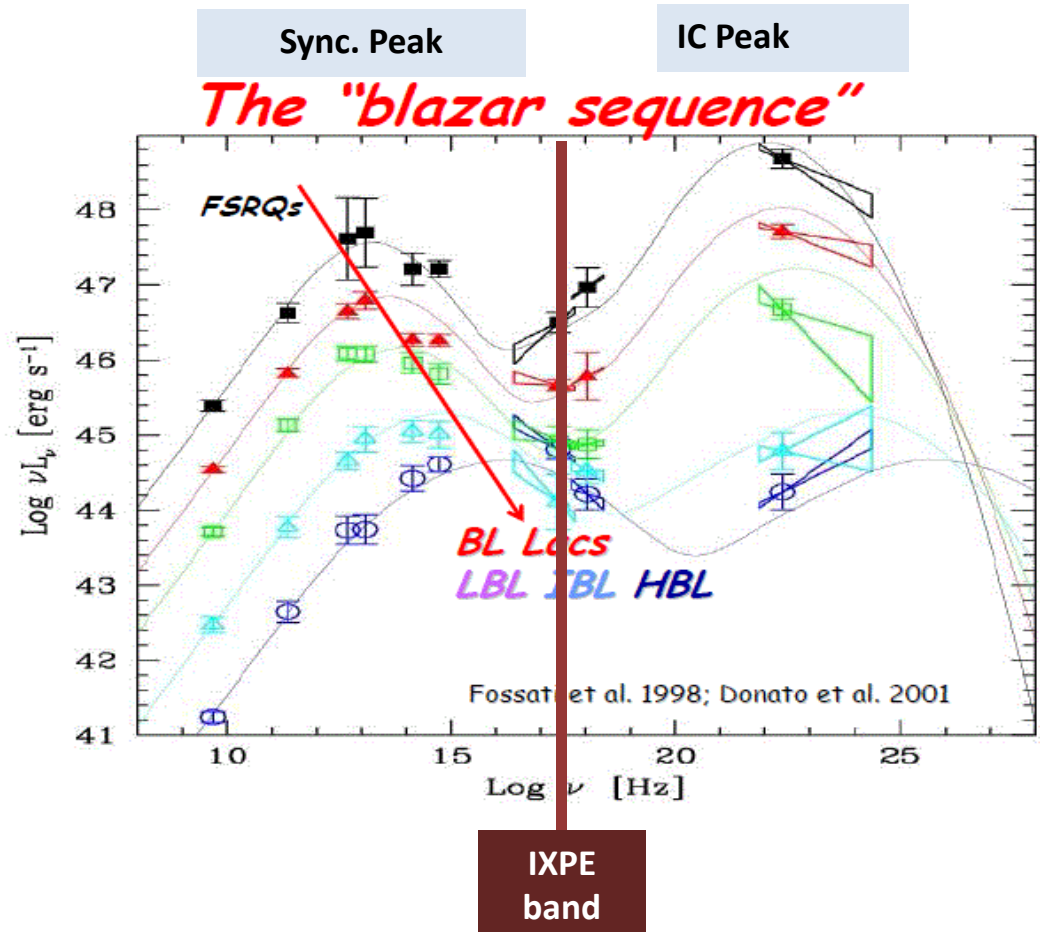
The polarization degree is related to the electron temperature in the jet.

In **synchrotron-dominated** X-ray Blazars, multi-wavelength polarimetry probes the structure of the magnetic field along the jet.

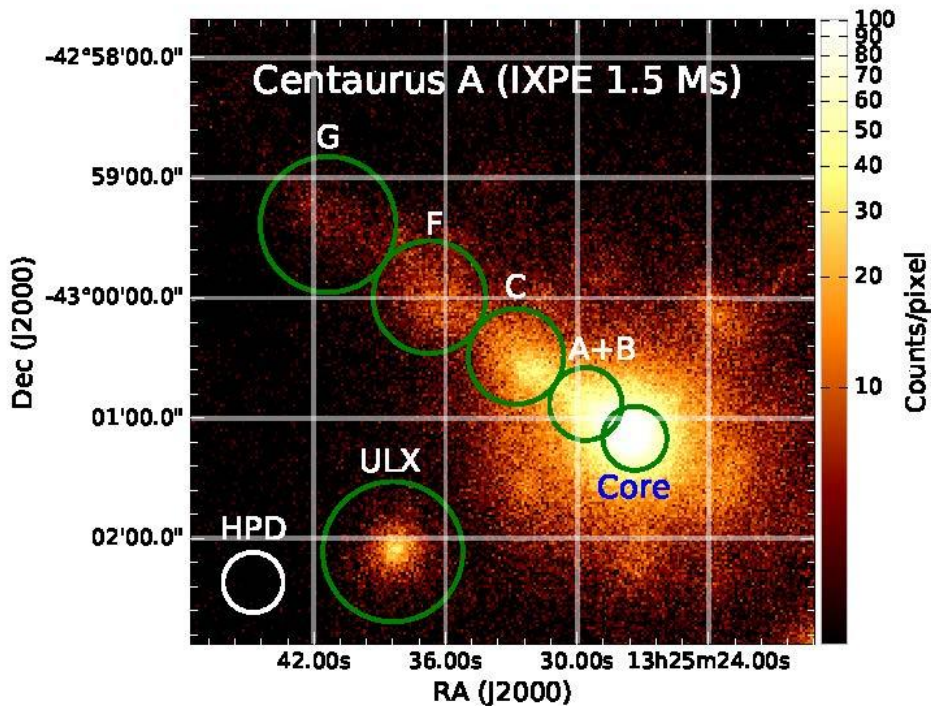
Models predict a larger and more variable polarisation in X-rays than in the optical.

Coordinated multi-wavelength campaigns are crucial for blazars.

Such campaigns (including polarimetry) are routinely organised and it will be easy for a X-ray polarimeter to join them.



... AND RADIOGALAXIES



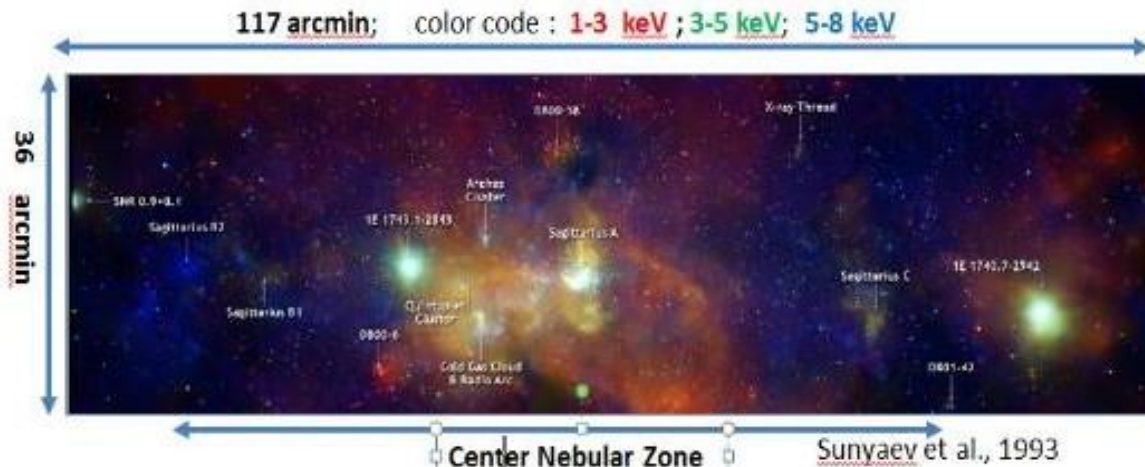
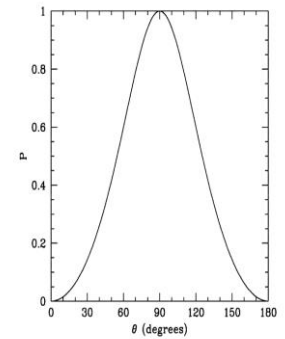
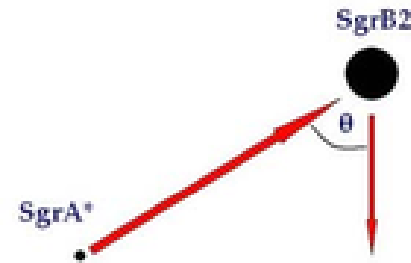
Region	MDP ₉₉
Core	0.4%
Jet	10.9%
Knot A+B	17.6%
Knot C	16.5%
Knot F	23.5%
Knot G	30.9%
ULX	14.8%

Includes effects of dilution by unpolarized diffuse emission

WAS THE GC ACTIVE A FEW CENTURIES AGO?

Galactic Center molecular clouds (MC) are known X-ray sources

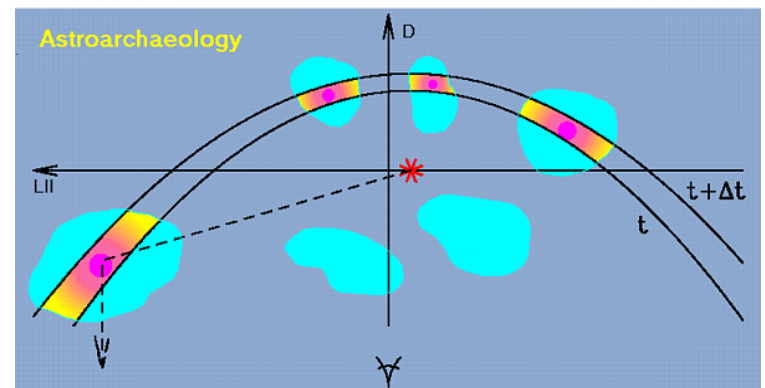
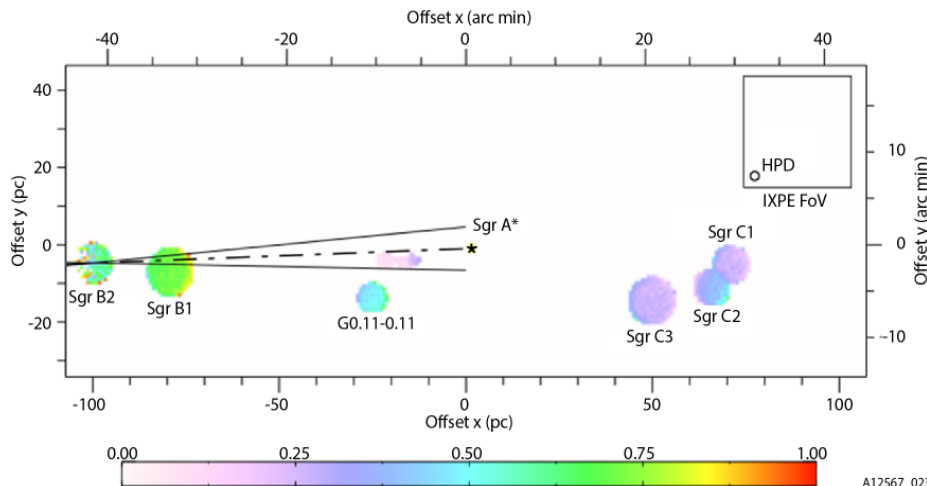
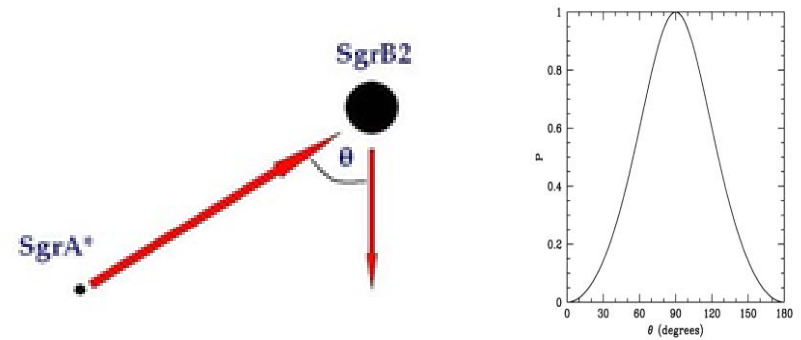
- Are MCs reflecting X-rays from Sgr A* ? (supermassive black hole in the GC)
 - X-radiation would be *highly polarized* perpendicular to plane of reflection and indicates the direction back to Sgr A*
 - Sgr A* X-ray luminosity was 10^6 larger \approx 300 years ago



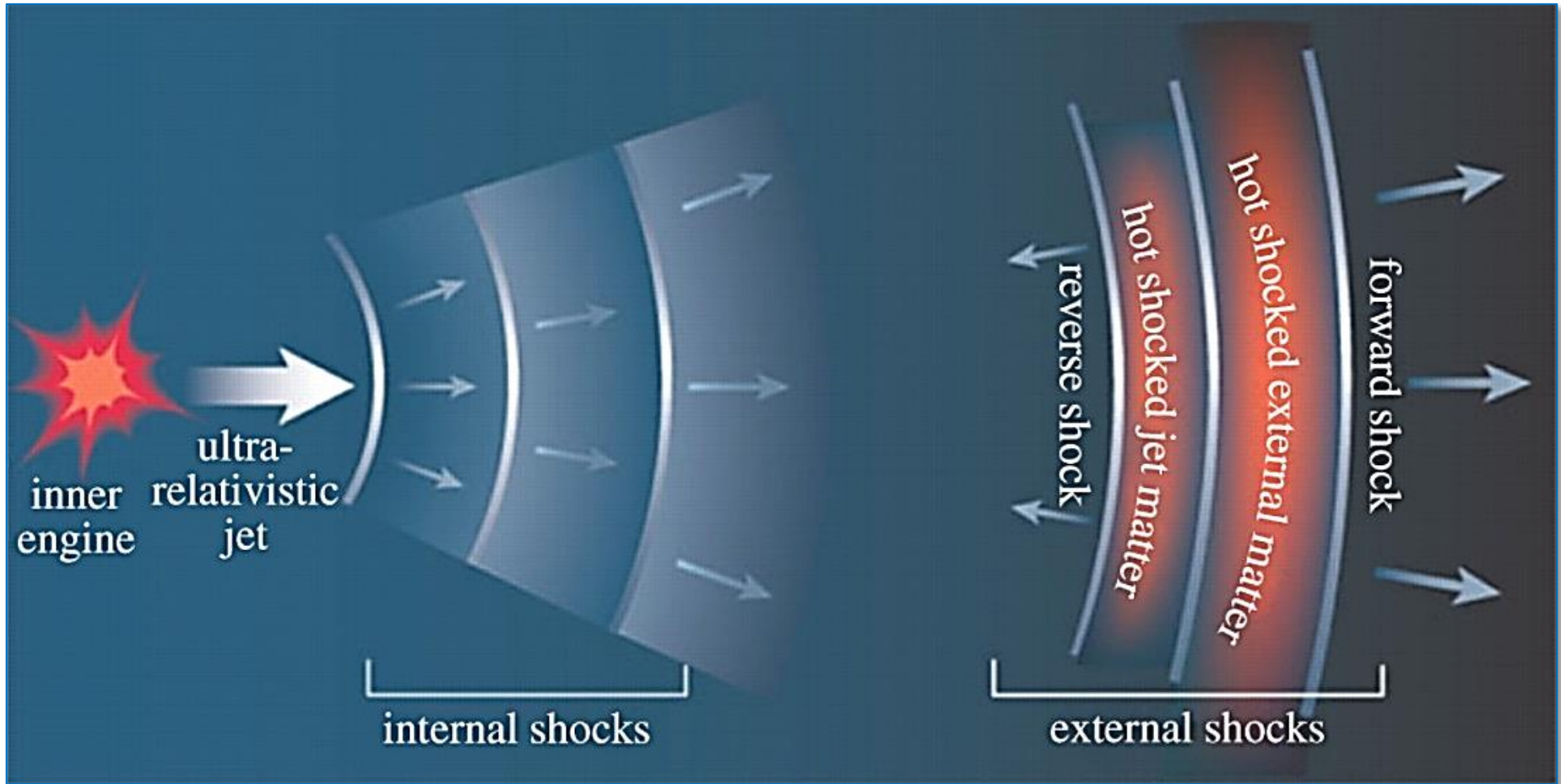
WAS THE GC ACTIVE A FEW CENTURIES AGO?

Galactic Center molecular clouds (MC) are known X-ray sources

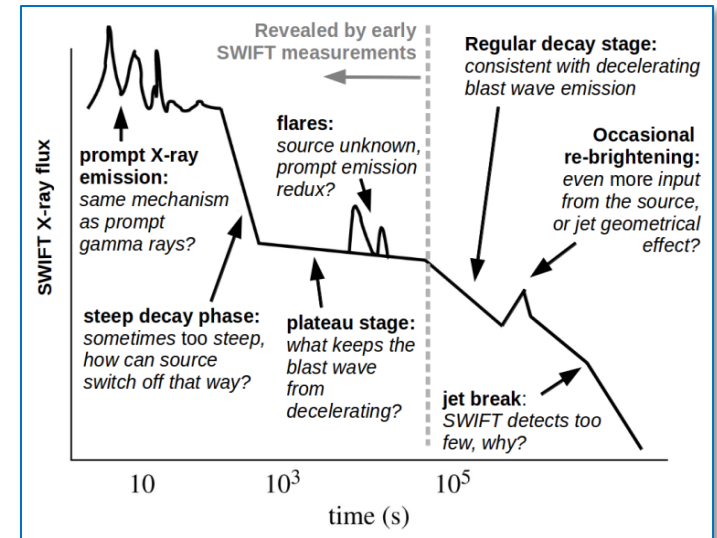
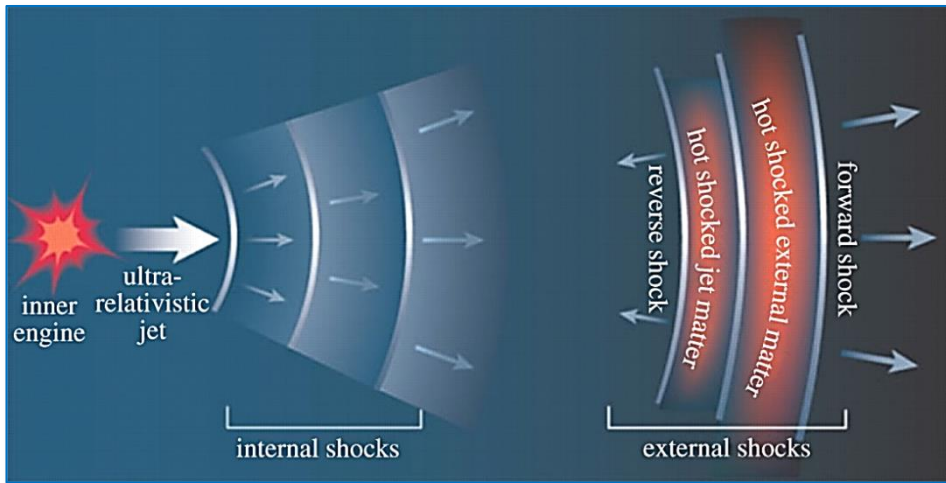
- Are MCs reflecting X-rays from Sgr A* ? (supermassive black hole in the GC)
 - X-radiation would be *highly polarized* perpendicular to plane of reflection and indicates the direction back to Sgr A*
 - Sgr A* X-ray luminosity was 10^6 larger ≈ 300 years ago



GAMMA-RAY BURSTS

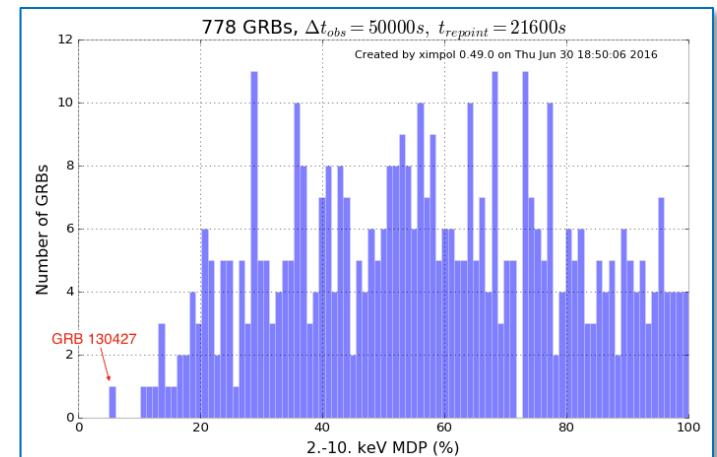


GAMMA-RAY BURSTS



X-ray polarimetry can answer several open questions:

- emission mechanism?
- the role of the magnetic field?
- composition of the expanding jets of GRBs during the late-time flares, plateau or re-brightening phases?

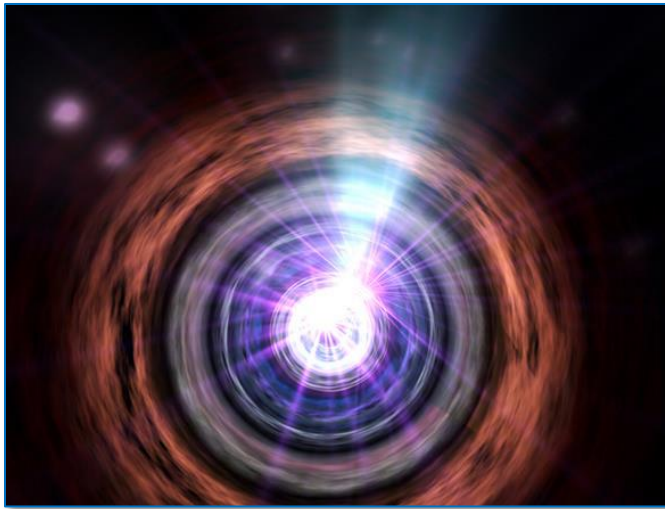




IXPE

Imaging
X-Ray
Polarimetry
Explorer

FUNDAMENTAL PHYSICS



Observing a sizeable sample of blazars at different redshifts, IXPE can search for energy-dependent **birefringence** effects.

They may put tighter constraints on QG theories.

Polarization variability detected for X-ray background sources of large, significantly magnetized regions (e.g. clusters of galaxies) may indicate the presence of **axion-like** particles.

These are one possible ingredient of dark matter.



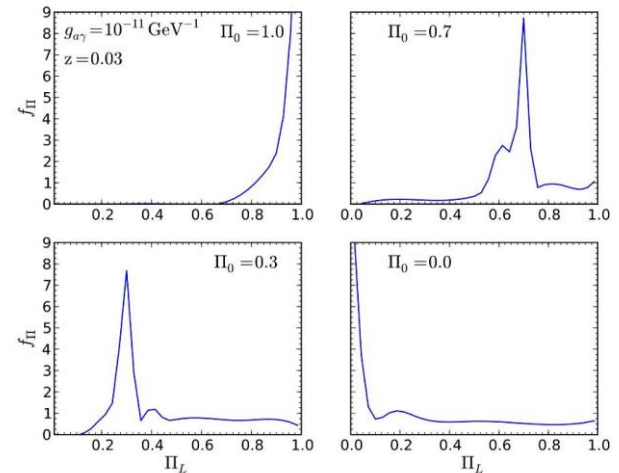


Observing a sizeable sample of blazars at different redshifts, IXPE can search for energy-dependent **birefringence** effects.

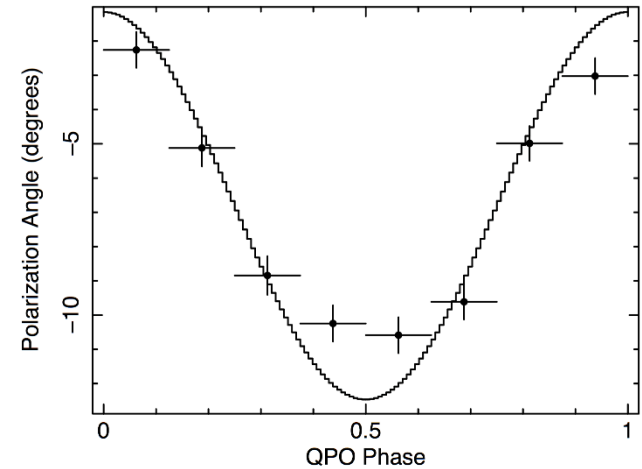
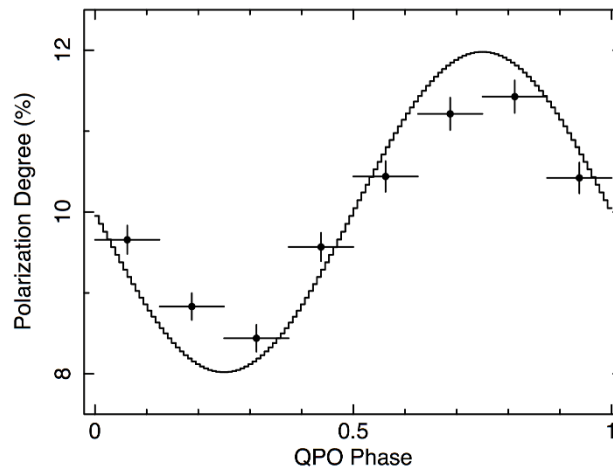
They may put tighter constraints on QG theories.

Polarization variability detected for X-ray background sources of large, significantly magnetized regions (e.g. clusters of galaxies) may indicate the presence of **axion-like** particles.

These are one possible ingredient of dark matter.



- Tidal Disruption Events: jet emission?
- QPO: Precession of the accretion flow

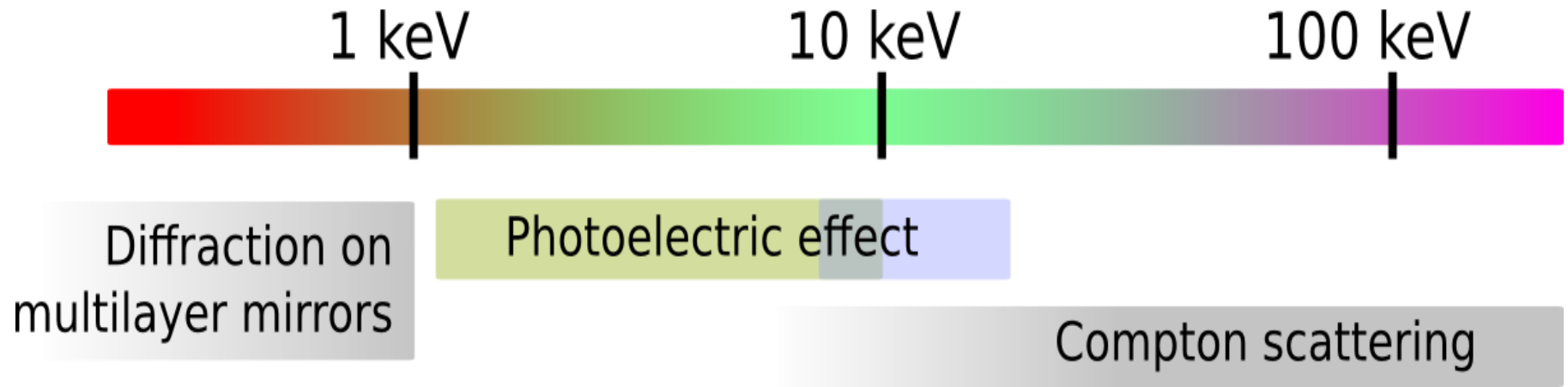


- ULX: geometry of the accretion flow



IXPE

Imaging
X-Ray
Polarimetry
Explorer



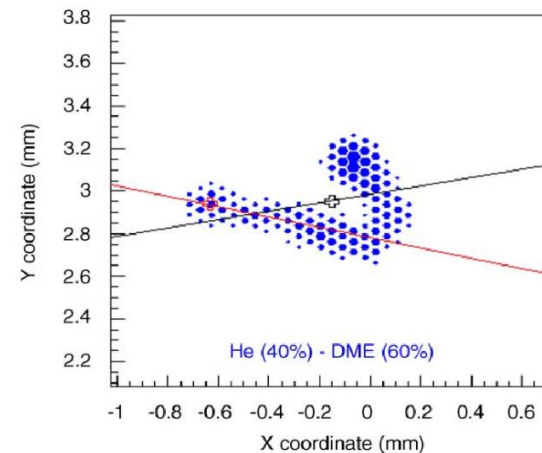
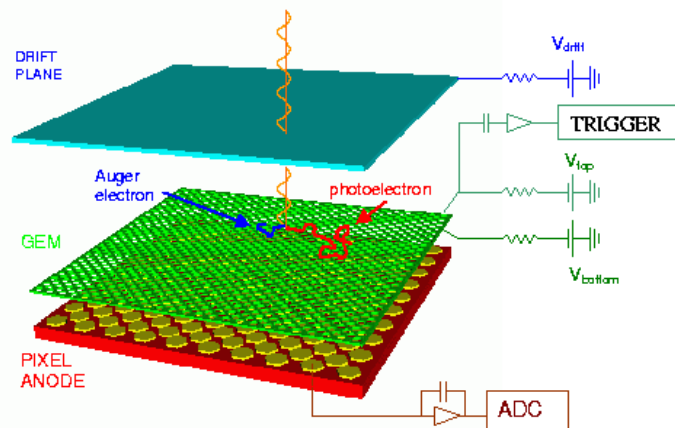


IXPE

Imaging
X-Ray
Polarimetry
Explorer

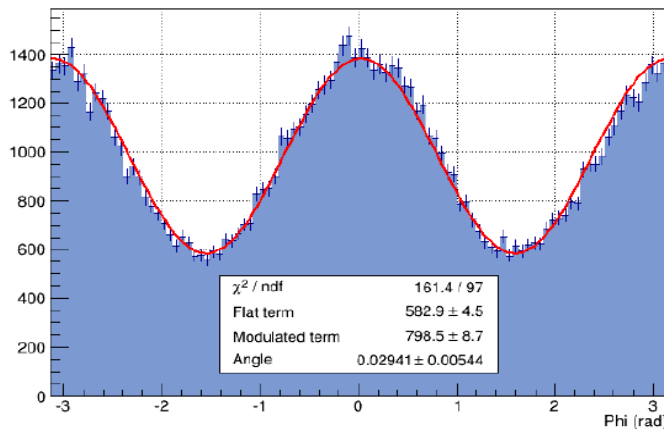
Scientific goal	Sources	< 1keV	1-10	> 10 keV
Acceleration phenomena	PWN	yes (but absorption)	yes	yes
	SNR	no	yes	yes
	Jet (Microquasars)	yes (but absorption)	yes	yes
Emission in strong magnetic fields	Jet (Blazars)	yes	yes	yes
	WD	yes (but absorption)	yes	difficult
	AMS	no	yes	yes
	X-ray pulsator	difficult	yes (no cyclotron)	yes
	Magnetar	yes (better)	yes	no
Scattering in aspherical geometries	Corona in XRB & AGNs	difficult	yes	yes (difficult)
	X-ray reflection nebulae	no	yes (long exposure)	yes
Fundamental Physics	QED (magnetar)	yes (better)	yes	no
	GR (BH)	no	yes	no
	QG (Blazars)	difficult	yes	yes
	Axions (Blazars, Clusters)	yes ?	yes	difficult

- **Mirror based on grazing incidence reflection**
 - Total collecting area: $>700 \text{ cm}^2$ at 3 keV
- **Photoelectric polarimeter based on GPD design**
 - Include a Filter & Calibration wheel with
 - Filters for specific observations (very bright sources, background)
 - Calibrations sources (polarized and unpolarized, gain)

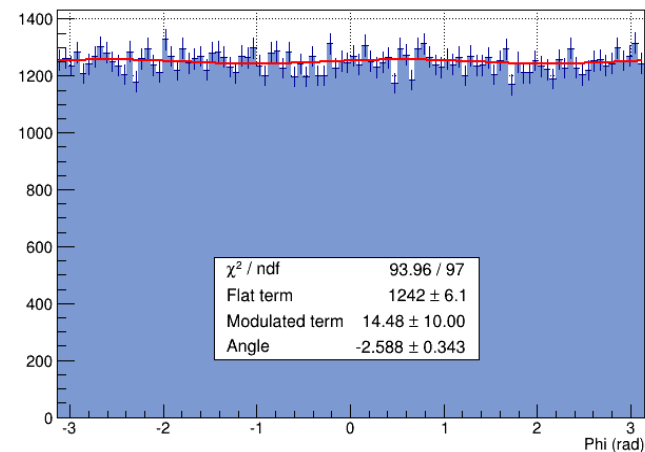


- **Mirror based on grazing incidence reflection**
 - Total collecting area: $>700 \text{ cm}^2$ at 3 keV
- **Photoelectric polarimeter based on GPD design**
 - Include a Filter & Calibration wheel with
 - Filters for specific observations (very bright sources, background)
 - Calibrations sources (polarized and unpolarized, gain)

(x,y)=(0.0,0.0)mm, 2nd step - 3.7 keV, 2769



Real modulation curve derived from the measurement of the emission direction of the photoelectron.



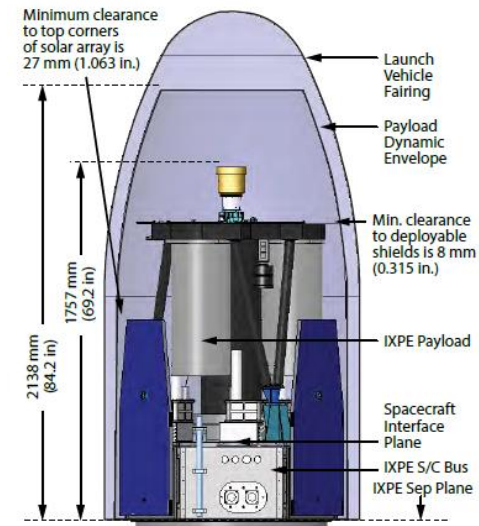
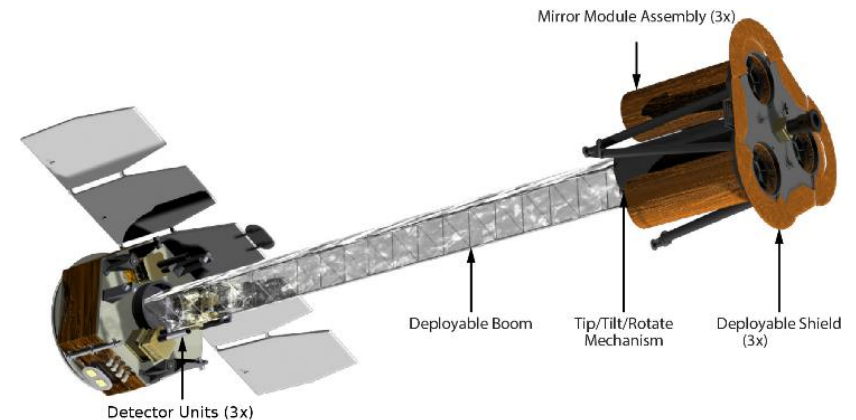
Residual modulation for unpolarized photons.

■ 3x Telescopes

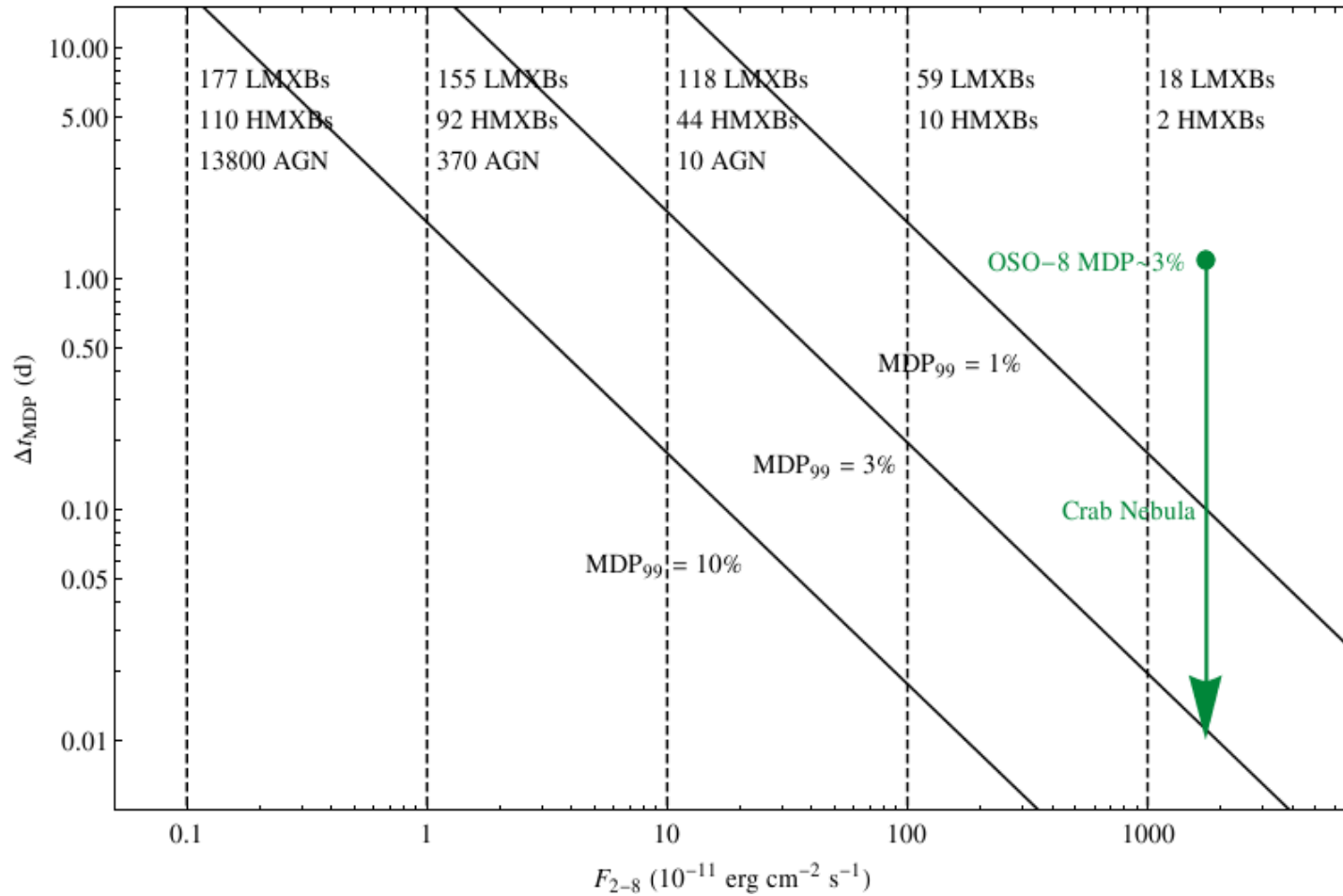
- 3x Mirror Units (MUs) + 3x Detector Units (DUs)
- A Detectors Service Unit (DSU) with built-in redundancy
- 4 m focal length, deployable boom and X-ray shield

■ Performance

- Polarization sensitivity: $MDP_{99\%} < 5.5\%$ in 1 day for flux of 10^{-10} ergs/cm²/sec
- Energy range: 2-8 keV
- Limit polarization: 0.5% (degree), 1 degree (angle)
- Angular resolution: better than 30 arcsec, field of view larger than 9 arcmin
- UTC synchronization: better than 250 μ s
- Energy resolution: better than 25%



OBSERVING PLAN



OBSERVING PLAN

Source name	F_{2-8} 10 ¹¹ cgs	MDP ₉₀ %	Δt day	Uncertainty σ_{ll} and σ_{ψ} for representative polarization measurements for indicated number of energy \times time or pulse phase \times spatial bins
Active Galactic Nuclei (AGN)				
Cen A radio galaxy	33.5	0.7	10.9	Core (4 bins) $ll \pm 0.5\%$, $\psi \pm 2.8^\circ$ (if $ll=5\%$) & Jet (4 bins) $ll \pm 1.5\%$, $\psi \pm 4.2^\circ$ (if $ll=10\%$)
NGC 4151 Seyfert	15.2	2.0	3.2	Survey
MCG-6-30-15 Seyfert	4.3	3.0	4.5	Survey
IC 4329A Seyfert	7.3	2.0	6.2	Survey
3C 273 quasar	6.5	2.0	7.4	(3 bins) $ll \pm 1.1\%$, $\psi \pm 6.5^\circ$ (if $ll=5\%$)
PKS 2155-304 blazar	7.3	2.0	5.5	(3 bins) $ll \pm 1.1\%$, $\psi \pm 3.3^\circ$ (if $ll=10\%$)
Mkn 501 blazar	3.1	3.0	6.8	(3 bins) $ll \pm 1.7\%$, $\psi \pm 4.9^\circ$ (if $ll=10\%$)
Mkn 421 blazar	27.2	2.0	1.6	(3 bins) $ll \pm 1.1\%$, $\psi \pm 3.3^\circ$ (if $ll=10\%$)
MCG-5-23-16 blazar	6.1	3.0	3.1	(3 bins) $ll \pm 1.7\%$, $\psi \pm 4.9^\circ$ (if $ll=10\%$)
1ES 1101-232 blazar	4.7	3.0	4.1	(3 bins) $ll \pm 1.7\%$, $\psi \pm 4.9^\circ$ (if $ll=10\%$)
BL Lac blazar	2.0	4.0	5.9	(3 bins) $ll \pm 2.3\%$, $\psi \pm 6.5^\circ$ (if $ll=10\%$)
Galactic Center				
Sgr B2	0.30	7.5	11.6	(3 bins) $ll \pm 4.3\%$, $\psi \pm 2.5^\circ$ (if $ll=50\%$), test hypothesis of Sgr A* reflection
Microquasars				
GRS 1915+105	1300	0.25	2.3	(4 bins) $ll \pm 0.2\%$, $\psi \pm 1.0^\circ$ (if $ll=5\%$), with energy, measure black-hole spin
LMC X-3 average	42	1.0	4.7	(4 bins) $ll \pm 0.7\%$, $\psi \pm 3.8^\circ$ (if $ll=5\%$); MDP = 3.1% in low state
GRO J1655 average	2020	0.4	0.5	(4 bins) $ll \pm 0.3\%$, $\psi \pm 1.5^\circ$ (if $ll=5\%$); MDP = 6.2% in low state
SS 433 average	18	1.5	4.4	(3 bins) $ll \pm 0.9\%$, $\psi \pm 4.9^\circ$ (if $ll=5\%$); MDP = 2.8% in low state
Cyg X-3 average	580	0.4	2.8	(4 bins) $ll \pm 0.3\%$, $\psi \pm 1.5^\circ$ (if $ll=5\%$); MDP = 0.7% in low state
Cyg X-1 average	1000	0.4	0.7	(4 bins) $ll \pm 0.3\%$, $\psi \pm 1.5^\circ$ (if $ll=5\%$); MDP = 0.6% in low state
Pulsar-Wind Nebulae (PWNe) + Pulsars (PSR)				
Crab PWNe + pulsar	1950	0.24	1.6	PWNe (25 bins) $ll \pm 0.4\%$, $\psi \pm 0.6^\circ$ (if $ll=20\%$), image magnetic structure Pulsar (9 bins) $ll \pm 2.6\%$, $\psi \pm 3.7^\circ$ (if $ll=20\%$), 34-ms pulse period, PWNe subtracted
Vela PWNe + pulsar	5.2	1.8	11.7	PWNe (18 bins) $ll \pm 2.6\%$, $\psi \pm 3.7^\circ$ (if $ll=20\%$), image magnetic structure Pulsar (2 bins) MDP = 19.9%, 89-ms pulse period, PWNe subtracted
MSH 15-52 + B1509-58	7.2	1.5	12.3	PWNe (18 bins) $ll \pm 2.6\%$, $\psi \pm 3.7^\circ$ (if $ll=20\%$), image magnetic structure Pulsar (9 bins) $ll \pm 3.1\%$, $\psi \pm 4.4^\circ$ (if $ll=20\%$), 151-ms pulse period, PWNe subtracted
G21.50-0.89 + J1833-103	3.9	3.0	5.6	Survey
Kes 75 + J1846-0258	1.4	4.0	8.9	Survey
N159A + B0540-69	2.2	4.0	5.2	Survey
Supernova Remnants (SNR)				
Cas A	116.0	0.35	11.6	(48 bins) $ll \pm 0.8\%$, $\psi \pm 4.6^\circ$ (if $ll=5\%$), image magnetic structure
Tycho	16.1	1.0	9.0	(18 bins) $ll \pm 1.4\%$, $\psi \pm 8.0^\circ$ (if $ll=5\%$), image magnetic structure
Kepler	2.9	2.5	9.4	(3 bins) $ll \pm 1.4\%$, $\psi \pm 8.2^\circ$ (if $ll=5\%$)
Kes 73	1.4	4.0	5.3	Survey
W49B	4.3	3.0	3.7	Survey



Source name	F_{2-8} 10^{11} cgs	MDP ₉₀ %	Δt day	Uncertainty σ_{II} and σ_{ψ} for representative polarization measurements for indicated number of energy \times time or pulse phase \times spatial bins
MSH 11-54	3.5	3.0	5.4	Survey
G 347.3-00.5 (W limb)	3.3	4.0	3.3	(3 bins) $II \pm 2.3\%$, $\psi \pm 6.5^\circ$ (if $I \neq 10\%$)
RCW 103 (shell)	1.0	5.0	6.8	(3 bins) $II \pm 2.8\%$, $\psi \pm 8.2^\circ$ (if $I \neq 10\%$)
Magnetars				
4U 0142+61	5.9	2.0	5.4	(9 bins) $II \pm 2.0\%$, $\psi \pm 1.1^\circ$ (if $I \neq 50\%$), 8.7-s pulse period, test vacuum birefringence
1RXS J170849.0-400910	4.3	2.5	5.6	(9 bins) $II \pm 2.5\%$, $\psi \pm 1.4^\circ$ (if $I \neq 50\%$), 11-s pulse period, test vacuum birefringence
Classical Accreting X-ray Pulsars (High-B X-ray Binaries)				
Cen X-3	341.	0.5	2.6	(27 bins) $II \pm 0.9\%$, $\psi \pm 1.2^\circ$ (if $I \neq 20\%$), 4.84-s pulse period
4U 0300-40	574.	0.5	1.5	(27 bins) $II \pm 0.9\%$, $\psi \pm 1.2^\circ$ (if $I \neq 20\%$), 283-s pulse period
SMC X-1	64.	1.0	3.8	(27 bins) $II \pm 1.7\%$, $\psi \pm 2.4^\circ$ (if $I \neq 20\%$), 0.71-s pulse period
Her X-1	87.	1.0	3.2	(27 bins) $II \pm 1.7\%$, $\psi \pm 2.4^\circ$ (if $I \neq 20\%$), 1.24-s pulse period
4U 1626-27	63.	1.0	2.3	(27 bins) $II \pm 1.7\%$, $\psi \pm 2.4^\circ$ (if $I \neq 20\%$), 7.7-s pulse period
IGR J1748-2446	78.	1.0	1.5	(27 bins) $II \pm 1.7\%$, $\psi \pm 2.4^\circ$ (if $I \neq 20\%$), 0.091-s pulse period
GRO J1744-28 bursting	1034.	0.5	0.8	(27 bins) $II \pm 0.9\%$, $\psi \pm 1.2^\circ$ (if $I \neq 20\%$), 0.467-s pulse period
4U 0115+634 outburst	254.	1.0	0.9	(27 bins) $II \pm 1.7\%$, $\psi \pm 2.4^\circ$ (if $I \neq 20\%$), 3.61-s pulse period
Accreting Millisecond X-ray Pulsars & other Low-B X-ray Binaries				
Sco X-1 *0.1 transmission	2250.	0.4	0.34	(5 bins) $II \pm 0.3\%$, $\psi \pm 1.7^\circ$ (if $I \neq 5\%$), with bright-source attenuating filter
Cyg X-2	987.	0.4	1.1	(5 bins) $II \pm 0.3\%$, $\psi \pm 1.7^\circ$ (if $I \neq 5\%$)
4U 1636-53 burster	352.	0.4	3.1	(27 bins) $II \pm 0.7\%$, $\psi \pm 3.9^\circ$ (if $I \neq 5\%$), 17-ms pulse period
4U 1728-337 burster	300.	0.4	3.6	(27 bins) $II \pm 1.7\%$, $\psi \pm 2.4^\circ$ (if $I \neq 5\%$), 28-ms pulse period
4U 1820-303 burster	710.	0.4	1.5	(5 bins) $II \pm 0.3\%$, $\psi \pm 1.7^\circ$ (if $I \neq 5\%$)
GS 1826-238 clocking	55.	1.0	3.4	(5 bins) $II \pm 0.7\%$, $\psi \pm 4.2^\circ$ (if $I \neq 5\%$)
J1908.4-3658 outburst	350.	0.4	2.3	(27 bins) $II \pm 0.7\%$, $\psi \pm 2.4^\circ$ (if $I \neq 5\%$), 25-ms pulse period



IXPE

Imaging
X-Ray
Polarimetry
Explorer

SUMMARY

**IXPE will reopen the X-ray polarimetry window,
providing crucial and unique information on the
physics and morphology of most classes of X-ray
sources**